

From Objects to Anywhere: A Holistic Benchmark for Multi-level Visual Grounding in 3D Scenes

Tianxu Wang¹, Zhuofan Zhang^{1,2}, Ziyu Zhu^{1,2}, Yue Fan¹,
Jing Xiong^{1,3}, Pengxiang Li^{1,4}, Xiaojian Ma¹, Qing Li^{1†}

¹BIGAI, ²Tsinghua University, ³Peking University, ⁴Beijing Institute of Technology

Project page: <https://anywhere-3d.github.io>

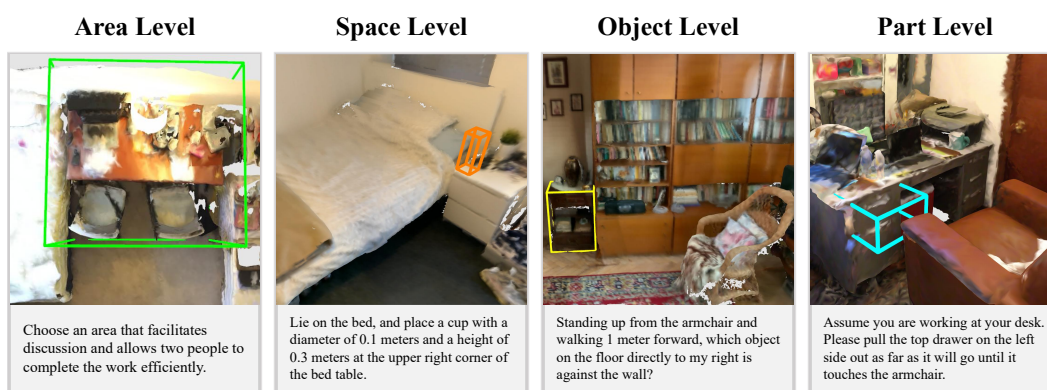


Figure 1: Multi-level Visual grounding in 3D Scenes: area, space, object, and part. Examples illustrate visual grounding of daily life expressions, from functional **areas** for collaborative study, to placing a cup on a nightstand in unoccupied **space**, referring to an **object** via its spatial distance from the armchair, or moving **part** of an object such as pulling out a drawer from a cabinet.

Abstract

3D visual grounding has made notable progress in localizing objects within complex 3D scenes. However, grounding referring expressions beyond objects in 3D scenes remains unexplored. In this paper, we introduce **Anywhere3D-Bench**, a holistic 3D visual grounding benchmark consisting of 2,632 referring expression-3D bounding box pairs spanning four different grounding levels: human-activity *areas*, unoccupied *space* beyond objects, individual *objects* in the scene, and fine-grained object *parts*. We assess a range of state-of-the-art 3D visual grounding methods alongside large language models (LLMs) and multimodal LLMs (MLLMs) on Anywhere3D-Bench. Experimental results reveal that space-level and part-level visual grounding pose the greatest challenges: space-level tasks require a more comprehensive spatial reasoning ability, for example, modeling distances and spatial relations within 3D space, while part-level tasks demand fine-grained perception of object composition. Even the best performance model, OpenAI o4-mini, achieves only 22.94% accuracy on space-level tasks and 33.68% on part-level tasks, significantly lower than its performance on area-level and object-level tasks. These findings underscore a critical gap in current models' capacity to understand and reason about 3D scenes beyond object-level semantics.

1 Introduction

When instructed to place a floor lamp next to an armchair, humans can visually ground it in the scene, estimating its base diameter and height, imagining its precise alignment with the armchair, and judging whether it fits naturally within the 3D environment. Humans can naturally perceive, reason about, and localize expressions to “anywhere” in 3D scenes. Yet can today’s 3D vision–language models ground free-form referring expressions to precise positions and dimensions in a 3D scene, especially when those expressions refer to regions beyond objects?

Existing 3D visual grounding models, pretrained on large 3D scene datasets, excel at aligning expressions to objects in a scene [7, 54, 2, 60, 57]. However, these models remain constrained to object-level alignment, with limited attention paid to the broader spatial regions beyond objects. Meanwhile, with the rapid development of Multimodal Large Language Models (MLLMs), an increasing number of studies have begun to explore their ability to perceive and reason about spatial intelligence from 2D images or videos [13, 6, 47, 41, 50, 17]. However, their ability to predict the positions and sizes of 3D bounding boxes corresponding to free-form referring expressions anywhere in 3D space, including both objects and regions beyond object boundaries, remains largely unexplored.

To bridge this gap, we introduce *Anywhere3D-Bench*, a holistic benchmark with 2,632 referring expression-3D bounding box pairs, categorized into four visual grounding levels: area, space, object, and part, as illustrated in Fig. 1. To the best of our knowledge, we are the first to propose a 3D visual grounding benchmark that spans multiple levels of grounding granularity, particularly on aligning expressions with 3D locations and sizes at **space level**. More diverse and illustrative examples can be found in Fig. 2. At each level, we design distinct types of referring expressions to evaluate models’ abilities to perceive and reason about various aspects of 3D space.

We conduct experiments on three categories of models on *Anywhere3D-Bench*: (1) LLMs with textual inputs, (2) MLLMs with both visual and textual inputs, and (3) 3D visual grounding specialist models. Evaluation results reveal that current models perform poorly on our benchmark, particularly on space-level and part-level tasks. Space-level tasks require modeling spatial relationships and distances in open space beyond individual objects, while part-level tasks demand first identifying the relevant object and then reasoning over its fine-grained structure to predict the appropriate bounding box size and position. Among all models, o4-mini—a strong MLLM with visual reasoning capabilities—achieves the best performance, yet still records only 22.94% accuracy on space-level and 33.68% on part-level tasks. These are significantly lower than its performance on the object-level (55.82%) and area-level (76.19%).

With visual inputs from video frames of the scene, MLLMs outperform their non-visual LLM counterparts, particularly on object-level and part-level tasks, where detailed visual cues, such as object appearance and structure, can be leveraged. In contrast, gains at the space level are more limited, suggesting that spatial relational reasoning in 3D space remains a significant bottleneck for MLLMs. Notably, LLMs and MLLMs generally outperform 3D visual grounding specialist models, especially on space-level tasks. This advantage can be attributed to their pretraining on large-scale image-text datasets, which endows them with stronger perceptual and understanding capabilities. Furthermore, their exposure to real-world knowledge enables a degree of commonsense reasoning, allowing them to infer 3D locations even beyond objects in the scene.

At the object level, our benchmark specifically assesses models’ ability to understand quantitative object sizes and inter-object distances, which are rarely emphasized in previous 3D visual grounding benchmarks. The best-performing 3D visual grounding model, Chat-Scene [23], achieves only 31.73% accuracy on the object-level task, substantially lower than the over 50%+ accuracy reported on benchmarks such as ScanRefer [7], highlighting current 3D visual grounding models’ limitations in reasoning about precise object dimensions and spatial distance.

To improve model performance on the two most challenging grounding levels: space-level and part-level, we introduce input enhancements as follows: (1) incorporate global coordinate information and object orientation to support a better understanding of spatial relationships, (2) select key video frames that convey critical visual cues aligned with the referring expression. While these enhancements lead to performance improvements on both space-level and part-level tasks, the gap with human performance remains substantial, highlighting that multi-level visual grounding demands more comprehensive perceptual and reasoning capabilities than current models possess.

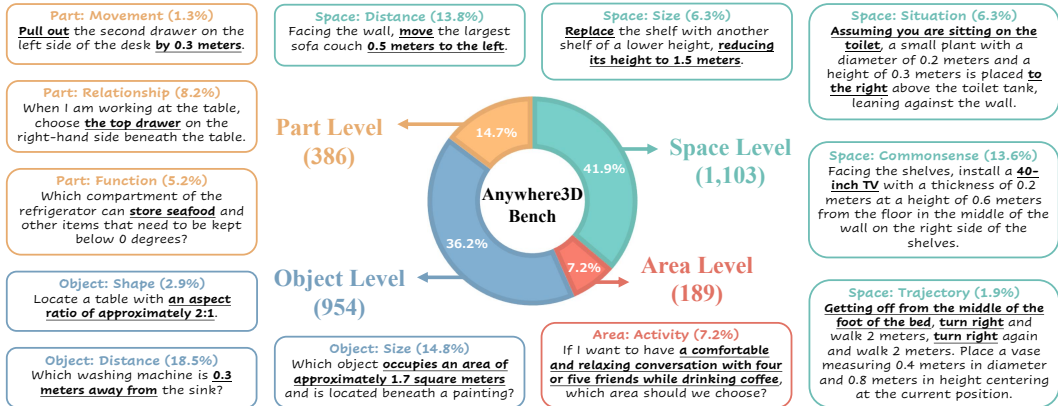


Figure 2: Multi-level visual grounding (Part, Space, Object, Area) with distinct expression types. **Emphasized segments** highlight phrases aligned with their respective expression type.

To summarize, our contributions are as follows:

- We introduce *Anywhere3D-Bench*, the first benchmark for multi-level 3D visual grounding that extends beyond the object level to cover four grounding levels in 3D scenes: area, space, object, and part.
- Experiments on *Anywhere3D-Bench* reveal that space-level and part-level visual grounding are the most challenging tasks. Even the best-performing model, o4-mini, with visual reasoning ability, struggles with these two tasks. Furthermore, compared to MLLMs, 3D visual grounding specialist models exhibit limited performance and poor generalization to space-level tasks.
- Additional spatial and visual cues boost performance on the two most challenging tasks: space-level and part-level. However, a significant gap still remains compared to human performance.

2 Anywhere3D Benchmark

Table 1: Comparison of Anywhere3D with existing visual grounding benchmarks (test splits). Anywhere3D expands grounding level to **area, space, object, and part**.

Benchmark	Area	Space	Object	Part	Test Source	Quality Check	# Scene	# Expression
ScanRefer	✗	✗	✓	✗	Human	✓	97	5,410
Nr3D	✗	✗	✓	✗	Human	✓	130	7,805
Sr3D	✗	✗	✓	✗	Template	✓	255	17,726
SceneFun3D	✗	✗	✗	✓	Human & Rephrasing	✓	85	1,265
ScanReason	✗	✗	✓	✗	GPT-4	✓	-	1,474
Anywhere3D (ours)	✓	✓	✓	✓	GPT-4	✓	276	2,632

As presented in Table 1, we introduce *Anywhere3D-Bench*, which consists of 2632 referring expression-3D bounding box pairs derived from 276 scenes from the validation sets of ScanNet [14], MultiScan [34], 3RScan [40], and ARKitScenes [4]. Inspired by how people refer to 3D scenes in everyday scenarios, we design four levels of grounding granularity and generate referring expressions specifically tailored to each level: Area Level (189), Space Level (1,103), Object Level (954), and Part Level (386). At each level, we design distinct types of referring expressions aiming at evaluating the models’ comprehensive capabilities, as further elaborated in the following section.

2.1 Multi-level Visual Grounding

We present the data distribution of *Anywhere3D-Bench* in Fig. 2, along with the representative examples of different types of referring expressions for each level.

Area Level Expressions belonging to the area level typically describe an indoor *Activity*, which requires the model to infer the related functional area composed of multiple objects and the space between them.

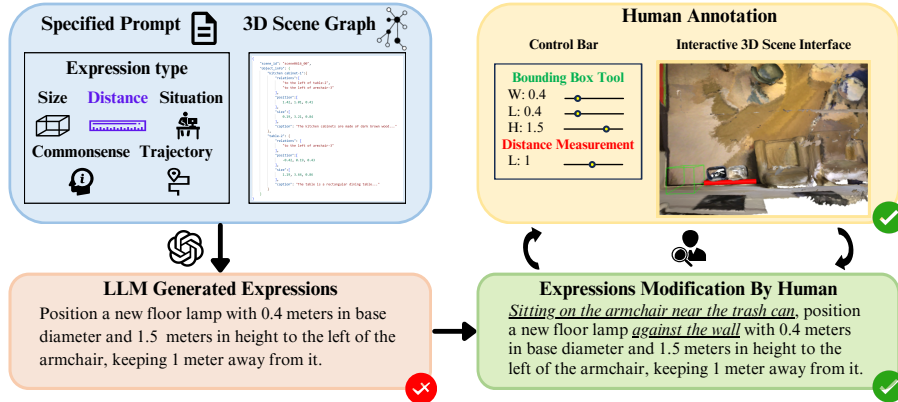


Figure 3: Data generation pipeline of Anywhere3D-Bench. We design specific prompts for different types of expression in four grounding levels. Human annotators are required to annotate the 3D bounding box and refine the GPT-generated expression until they precisely match.

Space Level Expressions in space level refer to spatial regions beyond objects in the 3D scene and are categorized into the following five types: *Size*: Expressions that require directly adjusting the size of an object or performing transformations on its dimension (e.g., length, width, height). This category evaluates models’ ability to interpret and manipulate quantitative object dimensions in 3D space. *Distance*: Expressions involving the relocation of an object or the placement of a new object at a specified distance from another. These test models’ ability to reason about quantitative spatial distances and relationships. *Situation*: Expressions involve imagining a scenario in a 3D scene from an egocentric perspective, as introduced in SQA3D [33]. This category evaluates models’ ability to understand the situation context and perspective within 3D environments. *Commonsense*: Expressions that include commonsense knowledge about object size (e.g., “40-inch TV”) or typical spatial locations in a scene (e.g., “room corner”). *Trajectory*: Expressions that specify the starting point and path of a trajectory, requiring the model to place an object at the endpoint and predict the location and size of the object.

Object Level Expressions refer to objects in the 3D scene, following the same setting as in prior works, such as ScanRefer and Nr3D [7, 1]. However, we place particular emphasis on models’ ability in reasoning about the quantitative understanding of object *Size*, *Shape*, and inter-object *Distance*.

Part Level Expressions refer to specific parts of objects in a 3D scene and can be categorized into the following three types: *Movement* requires models to predict the bounding box of an object part after certain movement, while *Relationship* and *Function* require models to predict a specific part of an object based on its spatial relationship or function.

2.2 Data Generation Pipeline

As shown in Fig. 3, the data generation pipeline of *Anywhere3D-Bench* involves referring expression generation guided by human-written prompts, along with iterative human annotation and verification. Notably, our annotation interface supports resizable and movable 3D bounding boxes, as well as a distance measurement tool, enabling precise annotation anywhere in the 3D space.

Referring Expressions Generation To enhance the diversity of referring expressions across various 3D scenes, we leverage GPT-4o [25] to generate expressions regarding different grounding levels as well as different types of expressions. For each scene, we first generate a 3D scene graph following SceneVerse [27]. Each scene graph contains ground-truth labels, IDs, and 3D bounding boxes of the objects, as well as object captions and inter-object relationships. We then prompt GPT-4o to generate referring expressions by providing the scene graph along with human-written prompts corresponding to a particular expression type and grounding level.

Human Annotation and Verification To ensure the quality of the benchmark, we construct a human-in-the-loop annotation and verification workflow. Annotators are provided with visualizations of the 3D scene, including ground-truth object labels and sizes. They are allowed to revise the

referring expressions and are required to annotate the corresponding 3D bounding boxes using an interactive interface equipped with a bounding box editor and distance measurement tool. A key requirement is emphasized throughout the workflow: **Each referring expression must be grounded exactly to one target 3D bounding box in the scene without ambiguity.**

All annotated expressions and 3D bounding boxes are subsequently verified by humans. Any annotation that does not meet the quality criteria is rejected and iteratively revised until it fully complies with the requirements.

3 Experiments and Results

3.1 Experimental Setting

Evaluation Metric In general, we adopt $\text{Acc}@k\text{IoU}$ as the evaluation metric following the standard setting of 3D visual grounding, where IoU is the Intersection over Union between the predicted 3D bounding box and the ground-truth bounding box formatted as $[center_x, center_y, center_z, size_x, size_y, size_z]$. To handle geometric ambiguities at multi-level visual grounding, we apply the following Eq. (1) for IoU. In our main paper, we set the threshold $t = 0.05(m)$, $k = 0.25$ and report $\text{Acc}@0.25\text{IoU}$. For evaluations under other k thresholds and further analysis of the IoU formulation, please refer to the Appendix.

$$\text{IoU} = \begin{cases} \text{IoU}_{xy}^{2D}, & \text{if level} = \text{“area”} \\ \text{IoU}_{\setminus i}^{2D} \cdot \mathbf{1}_{\{|center_i^{\text{gt}} - center_i^{\text{pred}}| < t \wedge size_i^{\text{pred}} < t\}}, & \text{if level} \neq \text{“area”}, \\ & size_i^{\text{gt}} < t, i \in \{x, y, z\} \\ \text{IoU}^{3D}, & \text{otherwise} \end{cases} \quad (1)$$

Baselines We evaluate three different types of models on our benchmark:

- **LLMs:** For each expression, the textual inputs of LLMs are formatted as a scene graph, consisting of ground-truth locations and sizes of objects, as well as object captions. The object captions are generated using Qwen2.5-VL-72B [3] conditioned on multiple object images and a guided captioning instruction (see Appendix for details). Closed-source models, including GPT-4.1 [35] and o4-mini [36], and open-source models, including thinking (Qwen3 [38], DeepSeek-R1-671B [19]) and non-thinking (Qwen2.5 [45, 3]) models are benchmarked.
- **MLLMs:** Following the setting in GPT4Scene [37], we incorporate a bird’s-eye view (BEV) image and eight uniformly sampled video frames with object markers as visual inputs, in addition to the textual inputs used in the LLM setting. Closed-source models, including GPT-4.1 and o4-mini, as well as open-source models, including LLaVA-OneVision [29], Qwen2.5-VL [3], and GPT4Scene [37] are evaluated.
- **3D Visual Grounding Models:** We also evaluate three state-of-the-art specialized 3D visual grounding models: 3D-VisTA [61], PQ3D [62], and Chat-Scene [23]. Since Chat-Scene does not provide 3D features for datasets other than ScanNet, its evaluation is limited to the ScanNet portion of our benchmark.

Human Evaluation We construct a human evaluation subset of 200 expressions through stratified random sampling across four levels to maintain their original distribution. Human evaluators are instructed to annotate the corresponding 3D bounding boxes for each expression. Evaluation results on this subset are reported using the same metric as mentioned above.

3.2 Main Results

Table 2 presents the overall results on our benchmark. Human performance substantially surpasses that of the best-performing model, o4-mini under the MLLM setting, particularly at the space level, indicating that current models fall far short of human-level 3D spatial intelligence.

Table 2: Results are presented in Acc@0.25IoU on Anywhere3D-Bench. *object bbox* in the table denotes the ground-truth object locations and sizes for simplicity. *Chat-Scene evaluation is only conducted on ScanNet. **Human performance is evaluated on a subset of 200 expressions obtained through stratified random sampling across four levels.

	Open Source	Area Level	Space Level	Object Level	Part Level	Overall
LLMs: <i>object bbox, captions</i>						
GPT-4.1	✗	76.19 ± 0.75	16.95 ± 0.77	48.00 ± 0.45	25.52 ± 0.92	33.72 ± 0.08
o4-mini	✗	71.96 ± 2.24	17.50 ± 0.25	48.69 ± 0.23	26.94 ± 0.74	34.10 ± 0.08
Qwen3-32B	✓	59.79 ± 3.70	12.15 ± 0.39	40.18 ± 0.48	19.17 ± 1.44	26.76 ± 0.44
Qwen2.5-72B	✓	60.14 ± 1.22	7.43 ± 0.33	33.30 ± 0.89	11.40 ± 2.07	21.17 ± 0.77
Qwen2.5-VL-72B	✓	56.35 ± 2.62	6.71 ± 0.38	29.19 ± 1.26	12.7 ± 2.57	19.30 ± 0.81
DeepSeek-R1-671B	✓	71.96 ± 1.40	13.93 ± 0.82	47.76 ± 0.12	24.79 ± 1.05	31.95 ± 0.53
MLLMs: <i>object bbox, captions, BEV, video frames</i>						
GPT-4.1	✗	81.48 ± 2.25	18.95 ± 0.64	53.88 ± 1.04	29.02 ± 0.73	37.58 ± 0.37
o4-mini	✗	76.19 ± 2.24	22.94 ± 0.90	55.82 ± 1.41	33.68 ± 0.37	40.24 ± 0.11
LLaVA-OneVision-7B	✓	19.58	2.27	8.81	4.66	6.23
Qwen2.5-VL-72B	✓	57.16 ± 0.50	10.21 ± 0.91	40.74 ± 0.34	17.79 ± 1.82	25.79 ± 0.67
GPT4Scene	✓	15.34	6.98	25.16	14.25	15.24
3D visual grounding models: <i>point clouds, video frames</i>						
PQ3D	✓	30.69 ± 0.92	7.98 ± 0.42	24.42 ± 0.18	20.90 ± 1.22	17.46 ± 0.10
3D-VisTA	✓	29.10 ± 0.92	7.16 ± 0.36	25.05 ± 0.46	20.64 ± 0.39	17.20 ± 0.02
Chat-Scene*	✓	49.10 ± 2.7	6.12 ± 0.50	31.73 ± 0.31	25.31 ± 0.62	23.41 ± 0.40
Human**	–	100.00	92.00	98.00	97.00	95.00

Area v.s. Space v.s. Object v.s. Part Grounding expressions at the space level is the most challenging task on our benchmark. This difficulty arises from the need to understand spatial relations and distance, situations, and reason over the absolute locations in 3D space beyond objects. The best-performing model, o4-mini with visual reasoning ability, only achieves 22.94% accuracy. Part-level visual grounding, though derived from object-level grounding, also poses significant challenges for all models. It requires the model to first identify the object to which the part belongs, and then reason about the part’s location and size based on spatial relationships, functions, and other contextual cues. In contrast, area-level and object-level grounding are relatively easier.

LLMs v.s. MLLMs Additional visual inputs, i.e., video frames and the bird’s-eye view image, consistently improve the performance of the same models (GPT-4.1, o4-mini, and Qwen2.5-VL-72B) when transitioning from the LLM setting to the MLLM setting. The performance gains are particularly notable at object level (8.19% on average) and part level (5.11% on average), as models can leverage visual inputs to access richer information about the object’s details, such as color and structure. However, improvements at the space level are much less pronounced (3.65% on average), suggesting that current MLLMs have limited ability to interpret spatial relationships in 3D space from 2D images.

MLLMs v.s. 3D Visual Grounding Models Both MLLMs and 3D visual grounding models are provided with visual inputs, along with the ground-truth bounding box locations and sizes. However, specialized 3D visual grounding models demonstrate limited performance, particularly at the space level, as they are restricted to predicting objects in the scene and lack generalizability for multi-level visual grounding tasks.

3.3 Detailed Analysis on Grounding Levels

Furthermore, we examine model performance across different types of referring expressions at each visual grounding level. Due to space limitations, we leave the analysis on area-level visual grounding to the Appendix.

Space Level We report the top-performing LLMs and MLLMs on different types of expressions at the space level, as illustrated in Fig. 4. Trajectory-based expressions are comparatively challenging, as they require a comprehensive understanding of spatial distance, relationships, and orientation. Expressions involving situation, distance, and commonsense also present difficulties, as they demand reasoning about spatial regions beyond objects in the scene. In contrast, size-related expressions are relatively easier: selecting the correct object, adjusting its size based on instructions, and performing positional refinements require less complex spatial perception and reasoning.

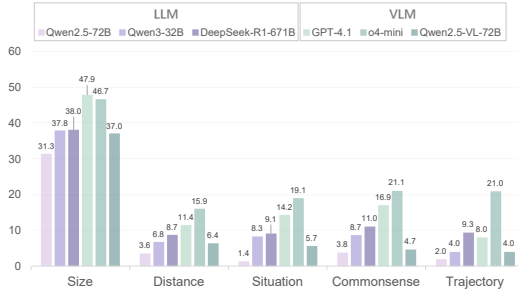


Figure 4: Results on different types of expressions on Space Level.

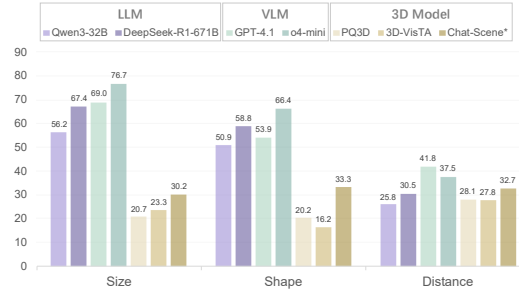


Figure 5: Results on different types of expressions on Object Level.

Object Level Fig. 5 demonstrates the performance of three types of expressions at object level. An interesting observation is that, compared to MLLMs, 3D visual grounding models exhibit a more balanced capability in interpreting object size, shape, and distances between objects. This may be attributed to the fact that 3D models are typically trained with inputs such as point clouds, which inherently encode spatial coordinates. In contrast, for MLLMs, object sizes are explicitly provided in the scene graph, which contributes to their stronger performance on size-related tasks, whereas estimating distances between objects requires both computation and commonsense reasoning.

Despite 3D visual grounding models’ relatively balanced ability to understand size and distance at the object level, they still underperform on our benchmark overall. Compared to the other visual grounding results reported in ScanRefer [7], which achieve about 50% accuracy, these models show a substantial performance drop on our benchmark. This suggests that reasoning about quantitative object size and inter-object distance remains a significant challenge for current 3D visual grounding approaches.

Part Level Fig. 7 shows the performance of top-performing models on different types of expressions at part level. Expressions involving dynamic movement present the greatest challenge for all models, as they must not only accurately identify the specific part of the object but also understand the object’s orientation to correctly predict the position of the bounding box after the movement. For expressions involving spatial relationships, even the best-performing MLLM model (o4-mini) achieves performance comparable to that of the 3D visual grounding model (Chat-Scene*), indicating that MLLMs still struggle with spatial relationships in 3D environments.

4 How Can We Improve MLLMs’ Ability on Multi-level Visual Grounding?

The above experimental results and analysis indicate that space-level and part-level visual grounding are the most challenging tasks in our benchmark. We select several representative examples from the second-best-performing model GPT-4.1, as the best-performing model o4-mini does not provide a reasoning process for detailed analysis. As illustrated in Fig. 6(a), (b), and (c), on space-level tasks, GPT-4.1 struggles with expressions involving situated contexts and trajectory, all of which require relational reasoning over object orientations, spatial directions, and spatial locations. On part-level tasks, as illustrated in Fig. 6(d) and (e), GPT-4.1 encounters difficulties in identifying specific parts from objects, due to the uniformly sampled video frames being insufficient to capture the key visual cues necessary for resolving the referring expressions. To address these challenges, we introduce visual and relational input enhancements to improve model performance, as detailed in the following section.

4.1 Visual Perception Enhancement

To further enrich the visual inputs, we incorporate key video frames **related to** the referring expressions in addition to the original visual inputs (i.e. **uniformly sampled** video frames and bird’s-eye view image). Specifically, given the original textual and visual inputs, we first prompt GPT-4.1 to output the candidate object IDs that it considers relevant to the referring expression. For each candidate object, we then select one video frame in which the object appears with the largest relative size and highlight it with a green 2D bounding box. Incorporating all these selected video frames

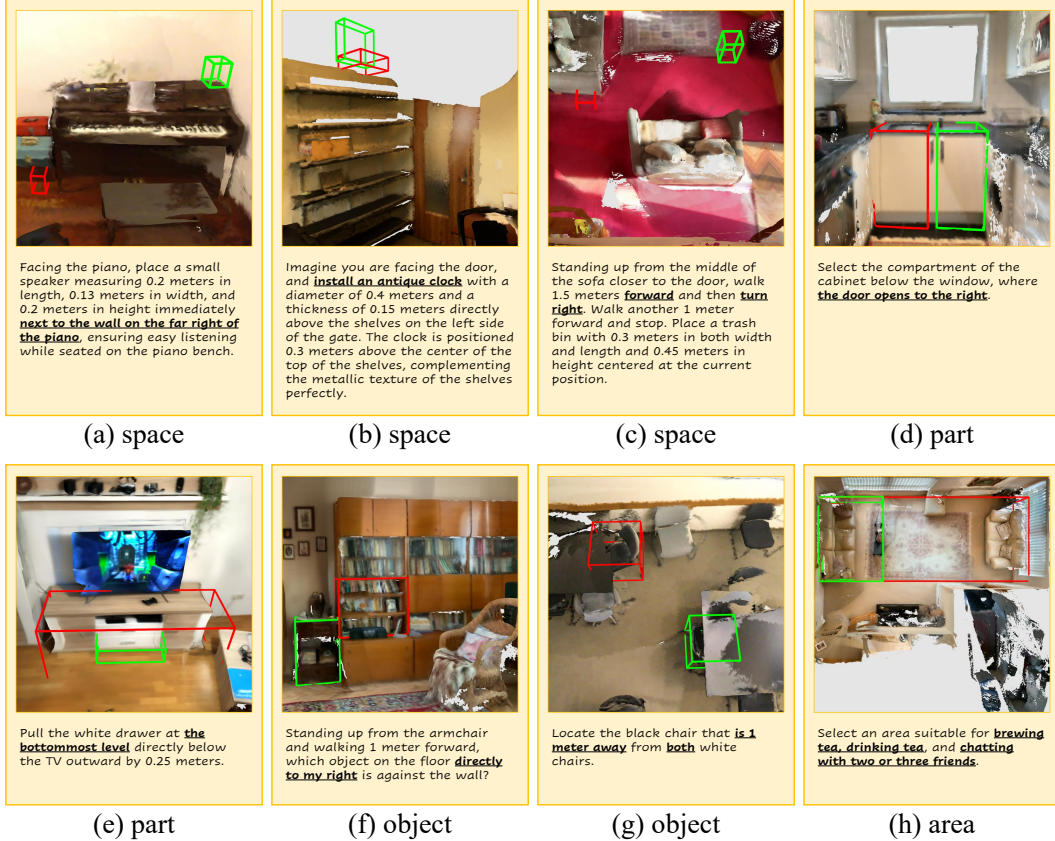


Figure 6: Qualitative examples from Anywhere3D-Bench. Green boxes indicate ground-truth, while red boxes show predictions from GPT-4.1. Examples (a)–(c): space-level; Examples (d) and (e): part-level; Examples (f) and (g): object-level; Example (h): area-level.

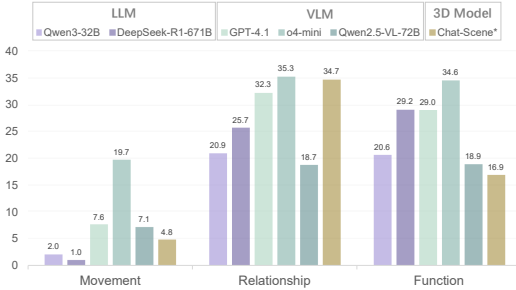


Figure 7: Results on different types of expressions on Part Level.

Table 3: Effect of the visual perception enhancement and the relational reasoning enhancement separately. Δ denotes the change in accuracy relative to GPT-4.1. The reported results are based on the human evaluation subset and averaged across three independent trials.

Method	Area	Space	Object	Part	Overall
<i>GPT-4.1</i>	86.67	15.29	54.29	33.33	37.00
Δ (GPT-keyframe)	4.44 ↓	2.75 ↑	2.86 ↓	8.90 ↑	1.00 ↑
Δ (Human-keyframe)	6.66 ↑	7.85 ↑	3.33 ↑	15.57 ↑	7.50 ↑
Δ (BEV-axes)	6.66 ↑	1.96 ↑	2.85 ↑	5.56 ↑	3.00 ↑
Δ (BEV-axes + ori.)	2.22 ↑	5.49 ↑	0.96 ↓	3.34 ↑	4.00 ↑

alongside the original inputs, we then require GPT-4.1 to predict the 3D bounding box corresponding to the expression.

Moreover, to illustrate the “upper bound” performance of incorporating additional selected video frames, we manually annotate the object IDs that humans consider relevant to each referring expression and select video frames accordingly. These video frames, combined with the original inputs, are then used as input to GPT-4.1.

As demonstrated in Table 3, incorporating additional related video frames improves GPT-4.1’s performance on *Anywhere3D-Bench*, particularly at the part level, which demands finer-grained object details. However, a performance gap remains between the objects proposed by the GPT-4.1

and those identified by humans, indicating GPT-4.1’s limitations in accurately selecting relevant objects.

4.2 Relational Reasoning Enhancement

To provide more spatial relation information to the MLLM, we adopt two approaches: scene-level enhancement and object-level enhancement. For scene-level enhancement, we overlay the x-axis and y-axis on the bird’s-eye view (BEV) image of the scene. For object-level enhancement, we incorporate object orientations—predicted by Orient-Anything [41]—into the textual scene graph input. To ensure consistency with the scene graph coordinate system, object orientations are discretized into +x, -x, +y, -y, or “not sure,” according to predictions from Orient-Anything (see Appendix for details).

As illustrated in Table 3, the combined use of scene-level and object-level enhancements improve GPT-4.1’s performance at the space level and part level. However, the accuracy remains far behind human performance. This highlights a substantial gap in spatial reasoning ability, even when models are provided with enriched spatial cues.

5 Related Work

3D Visual Grounding 3D vision-language learning establishes critical connections between natural language and 3D environments, enabling applications in augmented/virtual reality [8, 56] and embodied AI systems [16]. While this field encompasses diverse tasks such as 3D question answering [2, 59, 33] and dense captioning [11], 3D visual grounding—the precise localization of language-referred entities in 3D scenes—has emerged as a cornerstone for spatial intelligence. Despite the proliferation of benchmarks [7, 1, 54, 28, 60], existing datasets remain predominantly object-centric, constraining models to coarse-grained scene understanding. Recent efforts like SceneFun3D [15] partially address this limitation by introducing functional elements (e.g., handles, buttons), yet their scope remains narrow, excluding generic structural or semantic parts (e.g., “the left half of the desk”). Concurrently, while advanced methods [61, 62, 12, 20, 42, 32, 26, 58, 9, 48, 39, 43, 31, 55, 5, 46, 51] demonstrate progress in object-level localization, their capacity to interpret referrals at finer granularities remains underexplored. Our benchmark bridges this gap by introducing multi-granular localization across four hierarchical levels—*area*, *space*, *object*, and *part*—systematically evaluating model performance in complex, real-world 3D scene grounding.

Evaluating Multimodal Large Language Models on 3D Spatial Understanding Recent advancements in large language models (LLMs) have facilitated their integration into 3D domains. Early approaches, often termed “3D LLMs,” such as 3D-LLM, LEO, and Chat-Scene [21, 44, 30, 18, 22, 10, 24, 23], fine-tune LLMs to process embedded 3D object features. However, fine-tuning for 3D tasks is computationally expensive and risks catastrophic forgetting [52]. In contrast, GPT4Scene [37] demonstrates that multimodal large language models (MLLMs) can effectively tackle 3D understanding through simple visual prompting, bypassing the need for task-specific adaptation, which highlights the untapped potential of MLLMs in 3D intelligence. Concurrently, there is a growing interest in benchmarking off-the-shelf MLLMs on 3D tasks. *VSI-Bench* [47] evaluates 3D spatial reasoning in video understanding, while *All-Angles Bench* [49] tests MLLMs’ ability to establish correspondence between multi-view visual data. *ScanReQA* [53] further investigates how multimodal inputs affect spatial reasoning, comparing traditional 3D LLMs and MLLMs. Despite these efforts, the field has yet to systematically assess the 3D visual grounding abilities of MLLMs, leaving open questions about their precision in localizing and reasoning within complex spatial scenes.

6 Conclusion

In this paper, we present *Anywhere3D-Bench*, a novel and challenging benchmark that extends visual grounding to four levels in 3D scenes. Evaluation results show that even the best-performing MLLM, o4-mini, with visual reasoning capabilities, struggles with the two most difficult tasks—space-level and part-level grounding. This highlights the difficulty current MLLMs face in understanding and reasoning about 3D scenes based on 2D visual inputs. Furthermore, specialized 3D visual grounding models consistently underperform compared to MLLMs, particularly on space-level tasks, revealing their limited generalizability to multi-level grounding scenarios.

References

- [1] Panos Achlioptas, Ahmed Abdelreheem, Fei Xia, Mohamed Elhoseiny, and Leonidas Guibas. Referit3d: Neural listeners for fine-grained 3d object identification in real-world scenes. In *Computer Vision–ECCV 2020: 16th European Conference, Glasgow, UK, August 23–28, 2020, Proceedings, Part I 16*, pages 422–440. Springer, 2020.
- [2] Daichi Azuma, Taiki Miyanishi, Shuhei Kurita, and Motoaki Kawanabe. Scanqa: 3d question answering for spatial scene understanding. In *proceedings of the IEEE/CVF conference on computer vision and pattern recognition*, pages 19129–19139, 2022.
- [3] Shuai Bai, Keqin Chen, Xuejing Liu, Jialin Wang, Wenbin Ge, Sibong Song, Kai Dang, Peng Wang, Shijie Wang, Jun Tang, et al. Qwen2. 5-vl technical report. *arXiv preprint arXiv:2502.13923*, 2025.
- [4] Gilad Baruch, Zhuoyuan Chen, Afshin Dehghan, Yuri Feigin, Peter Fu, Thomas Gebauer, Daniel Kurz, Tal Dimry, Brandon Joffe, Arik Schwartz, et al. Arkitscenes: A diverse real-world dataset for 3d indoor scene understanding using mobile rgb-d data. In *Thirty-fifth Conference on Neural Information Processing Systems Datasets and Benchmarks Track (Round 1)*, 2021.
- [5] Chun-Peng Chang, Shaoxiang Wang, Alain Pagani, and Didier Stricker. Mikasa: Multi-key-anchor & scene-aware transformer for 3d visual grounding. In *CVPR*, pages 14131–14140, 2024.
- [6] Boyuan Chen, Zhuo Xu, Sean Kirmani, Brain Ichter, Dorsa Sadigh, Leonidas Guibas, and Fei Xia. Spatialvlm: Endowing vision-language models with spatial reasoning capabilities. In *Proceedings of the IEEE/CVF Conference on Computer Vision and Pattern Recognition*, pages 14455–14465, 2024.
- [7] Dave Zhenyu Chen, Angel X Chang, and Matthias Nießner. Scanrefer: 3d object localization in rgb-d scans using natural language. In *European conference on computer vision*, pages 202–221. Springer, 2020.
- [8] Dave Zhenyu Chen, Qirui Wu, Matthias Nießner, and Angel X Chang. D3net: A unified speaker-listener architecture for 3d dense captioning and visual grounding. In *ECCV*, pages 487–505. Springer, 2022.
- [9] Shizhe Chen, Pierre-Louis Guhur, Makarand Tapaswi, Cordelia Schmid, and Ivan Laptev. Language conditioned spatial relation reasoning for 3d object grounding. *Advances in neural information processing systems*, 35:20522–20535, 2022.
- [10] Sijin Chen, Xin Chen, Chi Zhang, Mingsheng Li, Gang Yu, Hao Fei, Hongyuan Zhu, Jiayuan Fan, and Tao Chen. LI3da: Visual interactive instruction tuning for omni-3d understanding reasoning and planning. In *CVPR*, pages 26428–26438, 2024.
- [11] Zhenyu Chen, Ali Gholami, Matthias Nießner, and Angel X Chang. Scan2cap: Context-aware dense captioning in rgb-d scans. In *CVPR*, 2021.
- [12] Zhenyu Chen, Ronghang Hu, Xinlei Chen, Matthias Nießner, and Angel X Chang. Unit3d: A unified transformer for 3d dense captioning and visual grounding. In *ICCV*, pages 18109–18119, 2023.
- [13] An-Chieh Cheng, Hongxu Yin, Yang Fu, Qiushan Guo, Ruihan Yang, Jan Kautz, Xiaolong Wang, and Sifei Liu. Spatialrgpt: Grounded spatial reasoning in vision-language models. *Advances in Neural Information Processing Systems*, 37:135062–135093, 2025.
- [14] Angela Dai, Angel X Chang, Manolis Savva, Maciej Halber, Thomas Funkhouser, and Matthias Nießner. Scannet: Richly-annotated 3d reconstructions of indoor scenes. In *Proceedings of the IEEE conference on computer vision and pattern recognition*, pages 5828–5839, 2017.
- [15] Alexandros Delitzas, Ayca Takmaz, Federico Tombari, Robert Sumner, Marc Pollefeys, and Francis Engelmann. Scenefun3d: fine-grained functionality and affordance understanding in 3d scenes. In *Proceedings of the IEEE/CVF Conference on Computer Vision and Pattern Recognition*, pages 14531–14542, 2024.
- [16] Jiafei Duan, Samson Yu, Hui Li Tan, Hongyuan Zhu, and Cheston Tan. A survey of embodied ai: From simulators to research tasks. *IEEE Transactions on Emerging Topics in Computational Intelligence*, 6(2): 230–244, 2022.
- [17] Yue Fan, Xiaojian Ma, Rujie Wu, Yuntao Du, Jiaqi Li, Zhi Gao, and Qing Li. Videoagent: A memory-augmented multimodal agent for video understanding. In *European Conference on Computer Vision*, pages 75–92. Springer, 2024.
- [18] Rao Fu, Jingyu Liu, Xilun Chen, Yixin Nie, and Wenhan Xiong. Scene-llm: Extending language model for 3d visual understanding and reasoning. *arXiv preprint arXiv:2403.11401*, 2024.

- [19] Daya Guo, Dejian Yang, Haowei Zhang, Junxiao Song, Ruoyu Zhang, Runxin Xu, Qihao Zhu, Shirong Ma, Peiyi Wang, Xiao Bi, et al. Deepseek-r1: Incentivizing reasoning capability in llms via reinforcement learning. *arXiv preprint arXiv:2501.12948*, 2025.
- [20] Zoey Guo, Yiwen Tang, Ray Zhang, Dong Wang, Zhigang Wang, Bin Zhao, and Xuelong Li. Viewrefer: Grasp the multi-view knowledge for 3d visual grounding. In *ICCV*, pages 15372–15383, 2023.
- [21] Yining Hong, Haoyu Zhen, Peihao Chen, Shuhong Zheng, Yilun Du, Zhenfang Chen, and Chuang Gan. 3d-llm: Injecting the 3d world into large language models. *Advances in Neural Information Processing Systems*, 36:20482–20494, 2023.
- [22] Yining Hong, Zishuo Zheng, Peihao Chen, Yian Wang, Junyan Li, and Chuang Gan. Multiply: A multisensory object-centric embodied large language model in 3d world. In *CVPR*, pages 26406–26416, 2024.
- [23] Haifeng Huang, Yilun Chen, Zehan Wang, Rongjie Huang, Runsen Xu, Tai Wang, Luping Liu, Xize Cheng, Yang Zhao, Jiangmiao Pang, et al. Chat-scene: Bridging 3d scene and large language models with object identifiers. In *The Thirty-eighth Annual Conference on Neural Information Processing Systems*, 2024.
- [24] Jiangyong Huang, Silong Yong, Xiaojian Ma, Xiongkun Linghu, Puhao Li, Yan Wang, Qing Li, Song-Chun Zhu, Baoxiong Jia, and Siyuan Huang. An embodied generalist agent in 3d world. In *Proceedings of the 41st International Conference on Machine Learning*, pages 20413–20451, 2024.
- [25] Aaron Hurst, Adam Lerer, Adam P Goucher, Adam Perelman, Aditya Ramesh, Aidan Clark, AJ Ostrow, Akila Welihinda, Alan Hayes, Alec Radford, et al. Gpt-4o system card. *arXiv preprint arXiv:2410.21276*, 2024.
- [26] Ayush Jain, Nikolaos Gkanatsios, Ishita Mediratta, and Katerina Fragkiadaki. Bottom up top down detection transformers for language grounding in images and point clouds. In *ECCV*, 2022.
- [27] Baoxiong Jia, Yixin Chen, Huangyue Yu, Yan Wang, Xuesong Niu, Tengyu Liu, Qing Li, and Siyuan Huang. Sceneverse: Scaling 3d vision-language learning for grounded scene understanding. In *European Conference on Computer Vision*, pages 289–310. Springer, 2024.
- [28] Shunya Kato, Shuhei Kurita, Chenhui Chu, and Sadao Kurohashi. Arkitscenerefer: Text-based localization of small objects in diverse real-world 3d indoor scenes. In *Findings of the Association for Computational Linguistics: EMNLP 2023*, pages 784–799, 2023.
- [29] Bo Li, Yuanhan Zhang, Dong Guo, Renrui Zhang, Feng Li, Hao Zhang, Kaichen Zhang, Peiyuan Zhang, Yanwei Li, Ziwei Liu, et al. Llava-onevision: Easy visual task transfer. *arXiv preprint arXiv:2408.03326*, 2024.
- [30] Zeju Li, Chao Zhang, Xiaoyan Wang, Ruilong Ren, Yifan Xu, Ruifei Ma, Xiangde Liu, and Rong Wei. 3dmit: 3d multi-modal instruction tuning for scene understanding. In *2024 IEEE International Conference on Multimedia and Expo Workshops (ICMEW)*, pages 1–5. IEEE, 2024.
- [31] Ziyang Lu, Yunqiang Pei, Guoqing Wang, Peiwei Li, Yang Yang, Yinjie Lei, and Heng Tao Shen. Scanneru: Interactive 3d visual grounding based on embodied reference understanding. In *AAAI*, pages 3936–3944, 2024.
- [32] Junyu Luo, Jiahui Fu, Xianghao Kong, Chen Gao, Haibing Ren, Hao Shen, Huaxia Xia, and Si Liu. 3d-sps: Single-stage 3d visual grounding via referred point progressive selection. In *CVPR*, 2022.
- [33] Xiaojian Ma, Silong Yong, Zilong Zheng, Qing Li, Yitao Liang, Song-Chun Zhu, and Siyuan Huang. Sqa3d: Situated question answering in 3d scenes. In *The Eleventh International Conference on Learning Representations*, 2022.
- [34] Yongsen Mao, Yiming Zhang, Hanxiao Jiang, Angel Chang, and Manolis Savva. Multiscan: Scalable rgbd scanning for 3d environments with articulated objects. *Advances in neural information processing systems*, 35:9058–9071, 2022.
- [35] OpenAI. Introducing gpt-4.1 in the api. <https://openai.com/index/gpt-4-1/>, 2025.
- [36] OpenAI. Openai o3 and o4-mini system card. <https://openai.com/index/o3-o4-mini-system-card/>, 2025.
- [37] Zhangyang Qi, Zhixiong Zhang, Ye Fang, Jiaqi Wang, and Hengshuang Zhao. Gpt4scene: Understand 3d scenes from videos with vision-language models. *arXiv preprint arXiv:2501.01428*, 2025.

- [38] Qwen Team. Qwen3: Think deeper, act faster. <https://qwenlm.github.io/blog/qwen3/>, 2025.
- [39] Xiangxi Shi, Zhonghua Wu, and Stefan Lee. Viewpoint-aware visual grounding in 3d scenes. In *CVPR*, pages 14056–14065, 2024.
- [40] Johanna Wald, Armen Avetisyan, Nassir Navab, Federico Tombari, and Matthias Nießner. Rio: 3d object instance re-localization in changing indoor environments. In *Proceedings of the IEEE/CVF International Conference on Computer Vision*, pages 7658–7667, 2019.
- [41] Zehan Wang, Ziang Zhang, Tianyu Pang, Chao Du, Hengshuang Zhao, and Zhou Zhao. Orient anything: Learning robust object orientation estimation from rendering 3d models. *arXiv preprint arXiv:2412.18605*, 2024.
- [42] Yanmin Wu, Xinhua Cheng, Renrui Zhang, Zesen Cheng, and Jian Zhang. Eda: Explicit text-decoupling and dense alignment for 3d visual grounding. In *CVPR*, pages 19231–19242, 2023.
- [43] Can Xu, Yuehui Han, Rui Xu, Le Hui, Jin Xie, and Jian Yang. Multi-attribute interactions matter for 3d visual grounding. In *CVPR*, pages 17253–17262, 2024.
- [44] Runsen Xu, Xiaolong Wang, Tai Wang, Yilun Chen, Jiangmiao Pang, and Dahua Lin. Pointllm: Empowering large language models to understand point clouds. In *ECCV*, pages 131–147. Springer, 2024.
- [45] An Yang, Baosong Yang, Beichen Zhang, Binyuan Hui, Bo Zheng, Bowen Yu, Chengyuan Li, Dayiheng Liu, Fei Huang, Haoran Wei, et al. Qwen2. 5 technical report. *arXiv preprint arXiv:2412.15115*, 2024.
- [46] Jianing Yang, Xuweiyi Chen, Shengyi Qian, Nikhil Madaan, Madhavan Iyengar, David F Fouhey, and Joyce Chai. Llm-grounder: Open-vocabulary 3d visual grounding with large language model as an agent. In *International Conference on Robotics and Automation (ICRA)*, pages 7694–7701. IEEE, 2024.
- [47] Jihan Yang, Shusheng Yang, Anjali W Gupta, Rilyn Han, Li Fei-Fei, and Saining Xie. Thinking in space: How multimodal large language models see, remember, and recall spaces. *arXiv preprint arXiv:2412.14171*, 2024.
- [48] Li Yang, Ziqi Zhang, Zhongang Qi, Yan Xu, Wei Liu, Ying Shan, Bing Li, Weiping Yang, Peng Li, Yan Wang, et al. Exploiting contextual objects and relations for 3d visual grounding. *NeurIPS*, 36, 2024.
- [49] Chun-Hsiao Yeh, Chenyu Wang, Shengbang Tong, Ta-Ying Cheng, Ruoyu Wang, Tianzhe Chu, Yuexiang Zhai, Yubei Chen, Shenghua Gao, and Yi Ma. Seeing from another perspective: Evaluating multi-view understanding in mllms, 2025.
- [50] Chun-Hsiao Yeh, Chenyu Wang, Shengbang Tong, Ta-Ying Cheng, Rouyu Wang, Tianzhe Chu, Yuexiang Zhai, Yubei Chen, Shenghua Gao, and Yi Ma. Seeing from another perspective: Evaluating multi-view understanding in mllms. *arXiv preprint arXiv:2504.15280*, 2025.
- [51] Zhihao Yuan, Jinke Ren, Chun-Mei Feng, Hengshuang Zhao, Shuguang Cui, and Zhen Li. Visual programming for zero-shot open-vocabulary 3d visual grounding. In *CVPR*, pages 20623–20633, 2024.
- [52] Yuexiang Zhai, Shengbang Tong, Xiao Li, Mu Cai, Qing Qu, Yong Jae Lee, and Yi Ma. Investigating the catastrophic forgetting in multimodal large language model fine-tuning. In *Conference on Parsimony and Learning (Proceedings Track)*, 2023.
- [53] Weichen Zhang, Ruiying Peng, Chen Gao, Jianjie Fang, Xin Zeng, Kaiyuan Li, Ziyu Wang, Jinqiang Cui, Xin Wang, Xinlei Chen, and Yong Li. The point, the vision and the text: Does point cloud boost spatial reasoning of large language models?, 2025.
- [54] Yiming Zhang, ZeMing Gong, and Angel X Chang. Multi3drefer: Grounding text description to multiple 3d objects. In *Proceedings of the IEEE/CVF International Conference on Computer Vision*, pages 15225–15236, 2023.
- [55] Yachao Zhang, Runze Hu, Ronghui Li, Yanyun Qu, Yuan Xie, and Xiu Li. Cross-modal match for language conditioned 3d object grounding. In *AAAI*, pages 7359–7367, 2024.
- [56] Yuqi Zhang, Han Luo, and Yinjie Lei. Towards clip-driven language-free 3d visual grounding via 2d-3d relational enhancement and consistency. In *CVPR*, pages 13063–13072, 2024.
- [57] Zhuofan Zhang, Ziyu Zhu, Pengxiang Li, Tengyu Liu, Xiaojian Ma, Yixin Chen, Baoxiong Jia, Siyuan Huang, and Qing Li. Task-oriented sequential grounding in 3d scenes. *arXiv preprint arXiv:2408.04034*, 2024.

- [58] Lichen Zhao, Daigang Cai, Lu Sheng, and Dong Xu. 3dvg-transformer: Relation modeling for visual grounding on point clouds. In *ICCV*, 2021.
- [59] Lichen Zhao, Daigang Cai, Jing Zhang, Lu Sheng, Dong Xu, Rui Zheng, Yinjie Zhao, Lipeng Wang, and Xibo Fan. Towards explainable 3d grounded visual question answering: A new benchmark and strong baseline. *IEEE Transactions on Circuits and Systems for Video Technology*, 2022.
- [60] Chenming Zhu, Tai Wang, Wenwei Zhang, Kai Chen, and Xihui Liu. Scanreason: Empowering 3d visual grounding with reasoning capabilities. In *European Conference on Computer Vision*, pages 151–168. Springer, 2024.
- [61] Ziyu Zhu, Xiaojian Ma, Yixin Chen, Zhidong Deng, Siyuan Huang, and Qing Li. 3d-vista: Pre-trained transformer for 3d vision and text alignment. In *Proceedings of the IEEE/CVF International Conference on Computer Vision*, pages 2911–2921, 2023.
- [62] Ziyu Zhu, Zhuofan Zhang, Xiaojian Ma, Xuesong Niu, Yixin Chen, Baoxiong Jia, Zhidong Deng, Siyuan Huang, and Qing Li. Unifying 3d vision-language understanding via promptable queries. In *European Conference on Computer Vision*, pages 188–206. Springer, 2024.

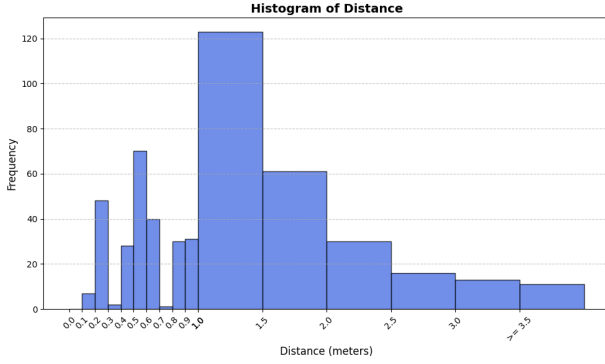


Figure A4: Distance Distribution of referring expressions at object level.

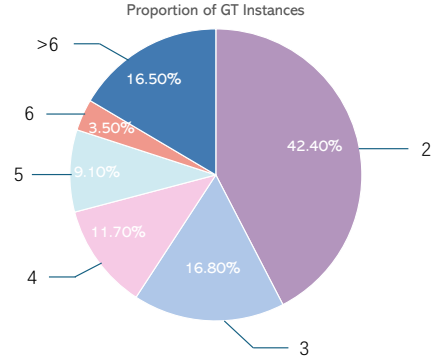


Figure A5: Distribution of object categories with two or more ground-truth instances at the object level. Only in these cases is the object label contained in the referring expression.

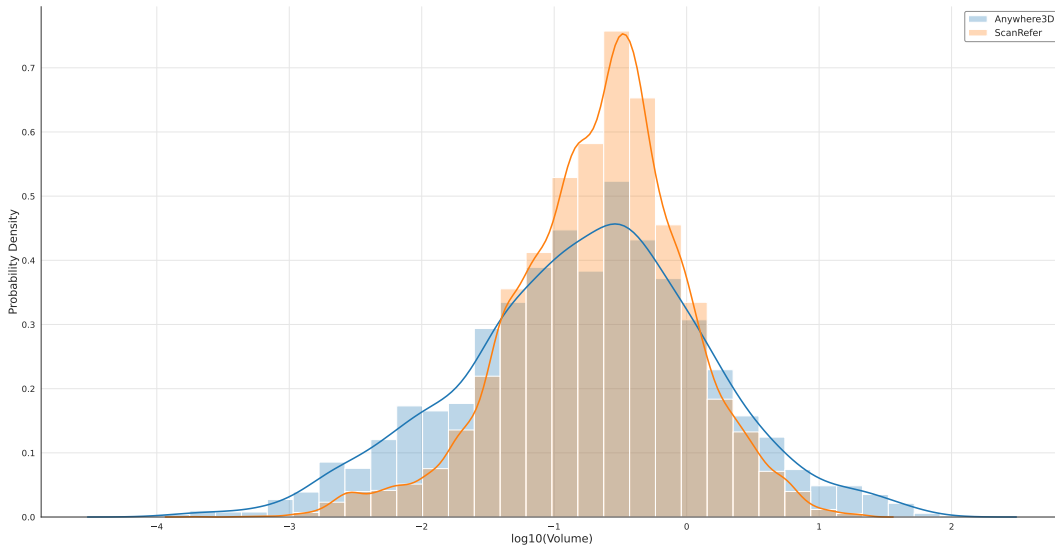


Figure A6: The target objects' volume distribution of Anywhere3D and ScanRefer. Logarithmic scaling is applied to the horizontal axis.

Anywhere3D expands grounding granularity beyond object-level annotations to include spaces, *parts* (typically small), and *areas* (typically large), enabling a more comprehensive evaluation of 3D visual grounding.

A.3 Data Generation Details

As demonstrated in Fig. A7, Fig. A8, and Fig. A9, we present the prompt messages for **distance-related** referring expressions generation at **space level** as an example.

```
messages = [{ 'role': 'system', 'content': System prompt }, { 'role': 'user', 'content': Scene graph of the scene to process }]
```

Figure A7: Prompt messages for referring expression generation with GPT-4o

You are now a helpful assistant that can generate diverse referring expressions that can be grounded to reasonable space in an indoor scene.

The scene is represented by a scene graph in JSON dictionary format. Each entity in the scene graph denotes an object instance, named '<category>-<ID>'. The 'caption' field describes the object's attributes, such as 'color', 'material', etc. The 'relations' field specifies the object's spatial relationships with other objects, defined from a viewpoint along the y-axis from positive to negative direction. The 'position' field contains the x, y, z coordinates of object's center in the scene. The 'size' field describes the width, length and height of the object's 3D bounding box. The numerical values of 'position' and 'size' correspond to units in meters. For example, from the scene graph:

```
""
"object_info": "kitchen counter-1": "relations": [{"below cabinet-4", "lower than soap dispenser-14", "lower than paper towel dispenser-15"}], "position": [1.27, 0.67, 0.9], "size": [0.74, 1.86, 0.26], "caption": "The kitchen counter is black granite with a stainless steel sink and faucet ... It is durable, easy to clean, and has a modern, sleek design that matches the stainless steel appliances in the kitchen.", ...
""
```

You can know that the center of "kitchen cabinets-5" is located in the x: 1.01, y: 0.37, z: 0.45, the "floor-6" has the width and length of 4.81 meters and 3.05 meters, the "microwave-8" is placed within the area of the "cabinets-3", the "cabinet-2" is to the left of "water cooler-7" viewing from +y axis to -y axis, the "water cooler-7" is 3 o'clock direction near the "cabinet-2" viewing from +y axis to -y axis.

Using the provided scene graph, design referring expressions that can be grounded to reasonable space in the 3D scene. There are two principles you need to read and follow very carefully:

1. Clarity: Each Referring Expression must be grounded exactly to one target 3D bounding box in space. Do not include the IDs of the objects in the referring expressions. Instead, use ordinal words, colors and relations to refer to different object instances of the same category. Describe the grounding position of the target 3D bounding box using only the surrounding objects to avoid causing confusion. Avoid using terms like "o'clock" to describe relations in referring expressions. Do not refer to existing objects with their corresponding positions in the scene! Additionally, consider whether the expressions require a specific viewpoint to ensure the target bounding box is clearly and uniquely identifiable. In some cases, specifying a viewpoint is necessary for achieving this level of precision. Please note that you don't need to stick to the original viewpoint in the scene graph (which is along the y-axis, from the positive to the negative), but if you specify a viewpoint, the spatial relations between objects in your referring expressions need to be consistent with the scene.

2. Distance Understanding Related: You should generate referring expressions in which the position of the bounding box should be explicitly specified based on its numerical distance from other objects in the scene. There are two main categories of referring expressions: existing object movement (move object already existed in the scene to another place) and new object increment (Add objects that not exist in the scene). For the category of 'new object increment', you may assume objects that not exist in the scene graph in each of the referring expressions. However, they should have reasonable sizes (For example, they should not exceed the boundary of the scene, not overlap with the existing objects.) and should be placed reasonably in the scene (For example, they are not allowed floating in the air). Also, you need to explicitly provide the sizes, i.e. (WIDTH, LENGTH, HEIGHT) or (DIAMETER, HEIGHT). You can also generate referring expressions beyond these categories that meet the principles above.

Below are some example referring expressions. Please note that these examples are derived from different scene graphs.

EXAMPLES

After you understand the contents above, I will provide a new scene graph below. Based on the two guiding principles and the examples provided above, generate referring expressions corresponding to the new scene graph.

Figure A8: System Prompts for generating distance-related referring expressions at the space Level using GPT-4o

1. Move the smaller trash bin next to the refrigerator to a spot 0.9 meters directly in front of the bicycle.
2. Facing the shower curtain, move the rug on the floor 0.3 meters to the right.
3. Pull the piano bench out by 0.5 meters to allow space for someone to sit and play the piano.
4. Move the trash can that is closest to the TV to the floor directly in front of the sink, placing it 0.7 meters away from the kitchen cabinet.
5. Shift the television on the wall 0.1 meters to the right.
6. Facing the tv, move the coffee table 0.55 meters to its left.
7. Place a basin with a radius of 0.25 meters and a height of 0.5 meters on the floor, centered 0.35 meters to the right of the sink.
8. Place a round coffee table 0.8 meter in front of the couch. The table has a diameter of 1.2 meter and a height of 0.7 meter.
9. Move the painting on the wall next to the bed downward so that the bottom of the painting is 1 meter above the floor.
10. Add a new table in front of the big sofa with dimensions 80 cm × 60 cm × 1 m. The table should be placed 1.5 meters away from the sofa and centered relative to it.
11. Sitting on the chair in front of the desk, place a notebook with 0.4m * 0.5m * 0.1m to the right of the laptop. Keep a distance of 0.15 meters between them.
12. Facing the whiteboard, add another foosball table in front of the old one, remaining 0.2 meters between the two tables.

Figure A9: [Examples in System Prompt](#) for GPT-4o referring expressions generations in distance-related expressions at space level.

A.4 Human Annotation and Verification Details

Fig. A10 and Fig. A11 illustrate the human annotation interface, which comprises four main components: a control bar, a 3D scene visualization module, an object list, and a referring expression editing box.

The control bar, located in the top-left corner, includes three primary tools: (1) a 3D bounding box annotation tool, (2) a distance measurement tool (i.e. *Scale Cylinder*), and (3) a coordinate axis visualization tool. Both the bounding box and distance measurement cylinder can be resized and repositioned using the control bar, and can also be interactively adjusted with the mouse. The dimensions ‘W’, ‘L’, and ‘H’ represent the lengths of the bounding box along the x-, y-, and z-axes, respectively.

The 3D scene visualization module, adapted from SQA3D, supports interactive operations such as zooming and rotating, allowing annotators to conduct detailed spatial exploration in the scene.

The object list, located in the top-right corner, displays all objects in the scene, along with their associated labels and sizes.

The referring expression editing box presents the expressions initially generated by GPT-4o and provides an interactive field for manual revision. Annotators can save their annotations or load previously saved ones as needed.

Overall, human annotation and verification process for all referring expressions cost approximately 900 USD and took around six weeks, including time for tool familiarization, pilot annotation, formal annotation, and human verification.

B Experiments and Results

B.1 Evaluation Metrics

In this section, we provide a detailed explanation of the IoU computation formula, as shown in Eq. (B1).



Figure A10: Human Annotation at part level: “Facing the mirror, pull out the top drawer in the first column from the right by 0.3 meters.”.

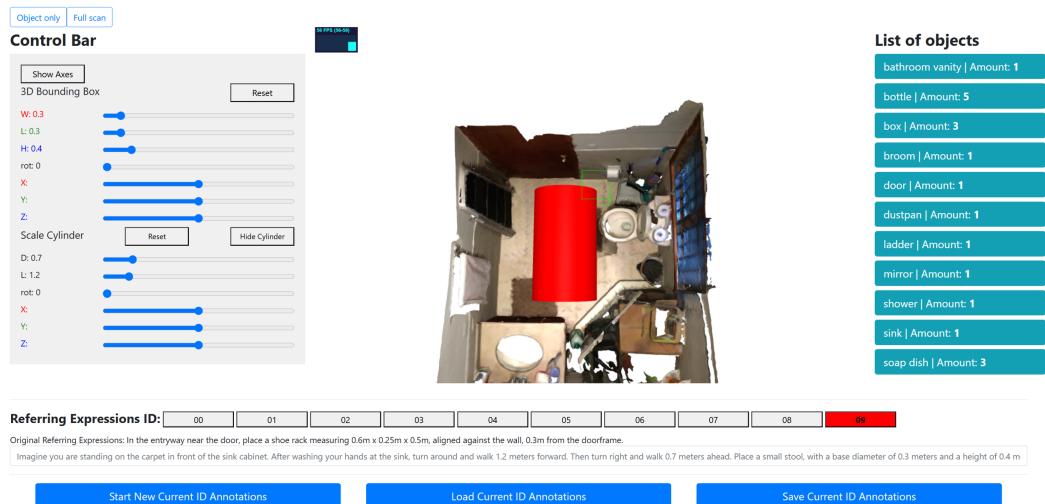


Figure A11: Human Annotation at space level: “Imagine you are standing on the carpet in front of the sink cabinet. After washing your hands at the sink, turn around and walk 1.2 meters forward. Then turn right and walk 0.7 meters ahead. Place a small stool, with a base diameter of 0.3 meters and a height of 0.4 meters, centered at your current position.” The scale cylinder serves as good annotation tool for trajectory annotation at space level.

$$\text{IoU} = \begin{cases} \text{IoU}_{xy}^{2D}, & \text{if level} = \text{“area”} \\ \text{IoU}_i^{2D} \cdot \mathbf{1}_{\{|center_i^{gt} - center_i^{pred}| < t \wedge size_i^{pred} < t\}}, & \text{if level} \neq \text{“area”}, \\ & size_i^{gt} < t, i \in \{x, y, z\} \\ \text{IoU}^{3D}, & \text{otherwise} \end{cases} \quad (\text{B1})$$

For the area level, we adopt 2DIoU on the horizontal plane as the evaluation metric, due to the inherent ambiguity in defining the vertical extent of the bounding box. For instance, it is unclear whether a study area comprising a desk and an office chair should extend vertically to the ceiling, as illustrated in Fig. B1.

Moreover, due to inevitable rendering artifacts in mesh visualization during human annotation, there can be small positional deviations—typically within a few centimeters. For certain objects with very small dimensions along one axis (e.g., a floor carpet that is only 0.02 meters thick(Fig. B2), or a wall clock with a thickness of 0.03 meters), directly computing the 3D IoU can lead to significantly distorted results, as the metric becomes overly sensitive to minor positional misalignments. To address this, we design a customized evaluation strategy for such objects.

Specifically, given a predefined threshold, if the ground-truth bounding box has a dimension smaller than this threshold along any axis (x, y, or z), and if the predicted bounding box satisfy both following conditions: (1) deviates from the ground-truth bounding box by less than the threshold along that axis in terms of position, and (2) is also smaller than the threshold in size along that axis, we consider the prediction to be accurate along that axis in both position and size. In this case, the IoU is computed as a 2D IoU over the remaining two axes only. We set the value of threshold to 0.05 meters in the paper.

Table B1 illustrates the ground-truth 3D bounding box and predicted 3D bounding box corresponding to Fig. B2. The height of the carpet(i.e., the size in the z-axis) is smaller than 0.05 meters. The predicted bounding box satisfies both of the conditions above, so the IoU between the predicted bounding box and the ground-truth bounding box will be the 2DIoU in the XY-Plane.

Table B1: 3D bounding box of ground-truth and prediction of GPT-4.1 corresponding to Fig. B2. The predicted 3D bounding box meets the criteria mentioned above, so IoU between ground-truth and prediction will be 2D IoU on the x-y plane ≈ 0.4696

	center_x	center_y	center_z	size_x	size_y	size_z
ground-truth	-0.01	-1.03	-0.03	1.8	1.2	0.02
prediction	-0.01	-0.68	0.01	1.2	1.8	0.02

B.2 Baseline Settings

To encourage diverse reasoning, we use the default temperature settings for all models, including GPT-4.1, o4-mini, Qwen3-32B, Qwen2.5-72B, Qwen2.5-VL-72B, DeepSeek-R1-671B, and DeepSeek-V3-671B. Each model is evaluated independently over three runs. The mean and standard deviation reported in the main paper and the Appendix are computed based on these three runs. Table B2 illustrates the specific versions of the LLMs and MLLMs used.

Table B2: Versions of LLMs and MLLMs.

Model	Qwen2.5-72B	Qwen3-32B	DeepSeek-R1-671B	DeepSeek-V3-671B	GPT-4.1	o4-mini	Qwen2.5-VL-72B
Version	2024-09-19	2025-04-29	2025-01-20	2024-12-26	2025-04-14	2025-04-16	2025-01-27

For both LLMs and MLLMs, we design system prompts tailored to each visual grounding level. The textual prompts consist of object ground-truth bounding boxes and captions generated by Qwen2.5-VL-72B (as further illustrated in Appendix B.3). In addition to textual inputs, MLLMs also receive a Bird’s Eye View (BEV) image and eight uniformly sampled video frames as visual inputs, following the setup of GPT4Scene. Fig. B3 and Fig. B4 show the textual inputs for LLMs at **space level**, while

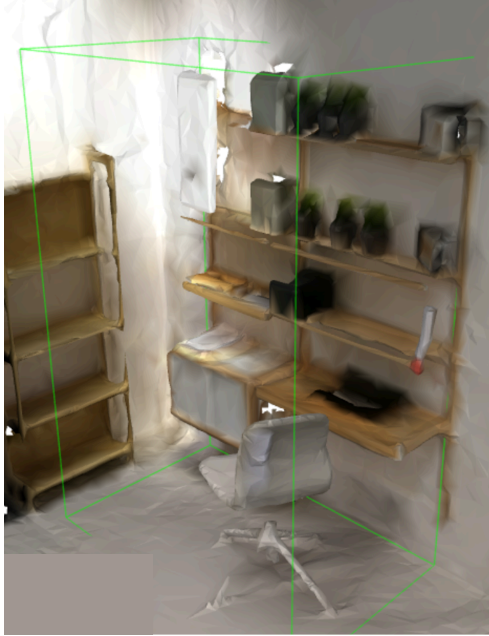


Figure B1: “Choose the area suitable for a study or home office setting.”



Figure B2: “Lay a new rectangular carpet on the floor directly in front of the sofa, ensuring it is 0.2 meters away from the sofa. The carpet should measure 1.2 meters wide, 1.8 meters long, and **0.02 meters thick.**”

Fig. B5 and Fig. B6 present the textual inputs for MLLMs at **space level**. An example of the BEV and video frames used as visual inputs for MLLMs is shown in Fig. B7.

```
messages = [{"role": "system", "content": "System prompt for specific grounding level"}, {"role": "user", "content": "Object_info": "Object_info": "Scene graph of the scene + "\n" + "Referring_expression": referring expression}]]
```

Figure B3: textual inputs for LLMs

Notably, we provide both LLMs and MLLMs with the ground-truth locations and sizes of objects. This design decouples object detection from 3D visual grounding, allowing us to specifically examine the models’ capabilities in perceiving, understanding, and reasoning within 3D scenes under ideal localization conditions.

After obtaining the model’s output, we extract the predicted 3D bounding box location and size using a combination of regular expressions and LLM-based parsing.

We utilize the fine-tuned checkpoints released by LLaVA-OneVision, GPT4Scene, PQ3D, 3D-VisTA, and Chat-Scene. Among them, GPT4Scene, PQ3D, 3D-VisTA, and Chat-Scene only produce object IDs corresponding to the referring expressions. Therefore, we derive the predicted 3D bounding boxes based on the size and location of the corresponding objects in the scene graph.

B.3 Object Caption Generation for Benchmarking

For LLMs and MLLMs, as outlined in Appendix B.2, the inputs include object captions generated by Qwen2.5-VL-72B. For each object in the scene, we prompt Qwen2.5-VL-72B to generate a descriptive caption using up to **five uniformly** sampled frames where the object is visible. To guide the captioning process, we annotate each frame with a green bounding box—projected from 3D space—to highlight the target object.

You are now a helpful assistant capable of grounding referring expressions to specific space within a 3D scene.

The scene is represented by a scene graph in JSON dictionary format. Each entity in the scene graph denotes an object instance, named '<object>-<ID>'. The 'position' field contains the x, y, z coordinates of object's 3D bounding box center in the scene. The 'size' field indicates the length of the object's 3D bounding box along the x, y, and z axes. Note that the x and y axes correspond to the horizontal plane, while the z axis corresponds to the vertical direction. The numerical values of 'position', 'size' correspond to units in meters. The "caption" field contains textual description of the object generated by a vision-language model (VLM) based on several images of the object. For example, from the scene graph:

```

"""
"object_info": "object-1": "position": [1.27, 0.67, 0.9], "size": [0.74, 1.86, 0.26], "caption": "The kitchen counter is black granite with a stainless steel ...", ...
"""

```

You can know that the center of "object-5" is located in the x: 1.01, y: 0.37, z: 0.45, the "object-6" has the length and width of 4.81 meters and 3.05 meters.

"Referring expressions" are natural language descriptions that point to a specific space within a 3D scene, which is represented by a scene graph.

For example, a referring expression like "Facing the bed, move the nightstand 0.3 meters backward." requires identifying the 3D bounding box of the nightstand after it has been moved 0.3 meters backward.

Your task is to determine the 3D bounding box corresponding to the referring expression and return the following details:

1. The x, y, z coordinates of the center of the bounding box.
2. The lengths of the bounding box along the x, y, and z axes.

After reviewing the information above, I will provide a new scene graph and a referring expression. Your task is to identify the 3D bounding box that corresponds to the referring expression within the new scene graph.

At the end of your response, please provide the following details for the identified 3D bounding box:

1. The x, y, z coordinates of its center, formatted strictly as: {xcoordinate: , ycoordinate: , zcoordinate: }
2. The length of the 3D bounding box along the x, y, and z axes, formatted strictly as: {xlength: , ylength: , zlength: }

Figure B4: System Prompts of LLMs textual inputs for space level

```

messages = [{ 'role': 'system', 'content': System prompt for specific grounding level }, { 'role': 'user', 'content': "Object_info": Scene graph of the scene + "\n" + "Referring_expression": referring expression + "\n" + "The subsequent images include a Bird Eye View image as the first, followed by 8 frames extracted from the scene video. Please return the center coordinates and sizes of predicted 3D bounding box STRICTLY following the instructed format."}]

```

Figure B5: textual inputs for MLLMs

The prompt instructs Qwen to describe the object within the bounding box, covering its category, material, color, shape, structure, function, and surrounding environment. The full prompt template is provided in Fig. B9.

An example is illustrated in Fig. B8

B.4 Main Results

Here we report Acc@0.5IoU and Acc@0.75IoU on *Anywhere3D-Bench* respectively, as presented in Table B3 and Table B4.

B.5 Thinking v.s. Non-thinking

We also test Deepseek-V3 as well as Qwen3 non-thinking modes for comparison between thinking models and non-thinking models. As shown in Table B5, Qwen3-32B thinking modes outperform non-thinking modes consistently, as DeepSeek-R1-671B outperforms DeepSeek-V3-671B consistently.

You are a helpful assistant skilled in grounding referring expressions to specific space within a 3D scene.

Each scene is represented by the following elements:

1. scene graph: a JSON-formatted dictionary that enumerates all objects in the scene. Each entity in the scene graph denotes an object instance, named '<object>-<ID>'. For each object, the 'position' field contains the x, y, z coordinates of the center of its 3D bounding box. The 'size' field indicates the length of the 3D bounding box along the x, y, and z axes. The x and y axes represent the horizontal plane, while the z axis represents the vertical direction. The values in 'position' and 'size' are in meters. The "caption" field contains textual description of the object generated by a vision-language model (VLM) based on several images of the object.
2. Bird's Eye View (BEV) Image: A top-down view of the scene, where objects' IDs are labeled in the image.
3. 2D Images: A set of 8 frames captured at equal intervals from the scene video. Each frame contains several objects with their object IDs labeled within red circles.

Note that object IDs are consistent across the scenegraph, 2D images, and BEV image.

Referring expressions are natural language descriptions that point to specific space within the 3D scene.

For example, a referring expression like "Facing the bed, move the nightstand 0.3 meters backward." requires identifying the 3D bounding box of the nightstand after it has been moved 0.3 meters backward.

Your task is to determine the position and size of the 3D bounding box corresponding to the referring expression.

After reviewing the information, I will provide a scene graph, 2D images, and a BEV image of a new scene, along with a referring expression. Your goal is to identify the 3D bounding box that corresponds to the referring expression.

At the end of your response, please provide the following details for the identified 3D bounding box:

1. The x, y, z coordinates of its center, strictly formatted as: xcoordinate: , ycoordinate: , zcoordinate:
2. The length of the 3D bounding box along the x, y, and z axes, strictly formatted as: {xlength: , ylength: , zlength: }

Figure B6: System Prompts of MLLMs textual inputs for space level

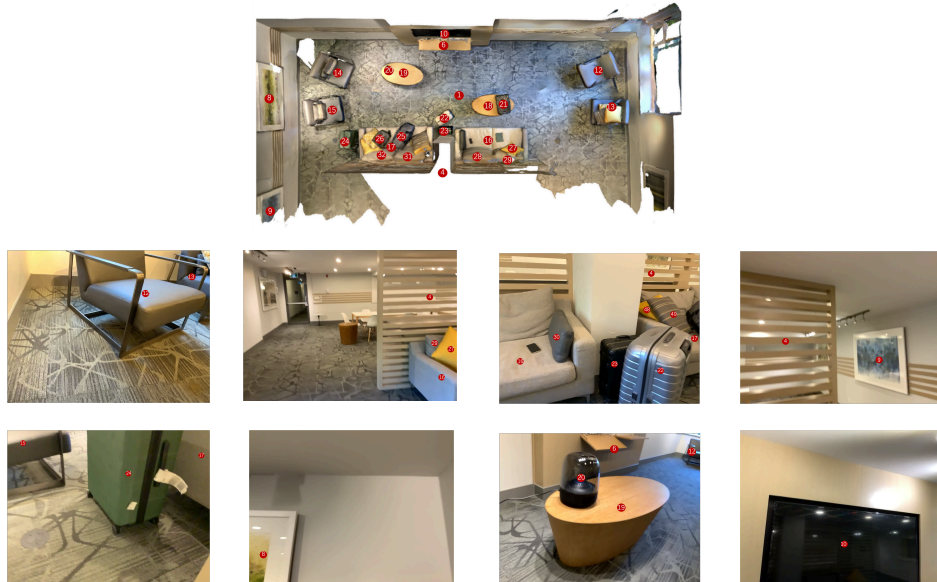


Figure B7: GPT4Scene Bird's Eye View (BEV) and eight uniformly sampled video frames from MultiScan Scene00109_00. The image at the top depicts the BEV, while the 2 × 4 grid below shows the video frames. In both the BEV and the video frames, object labels are marked with red circles to indicate object locations, following the visual input in GPT4Scene.

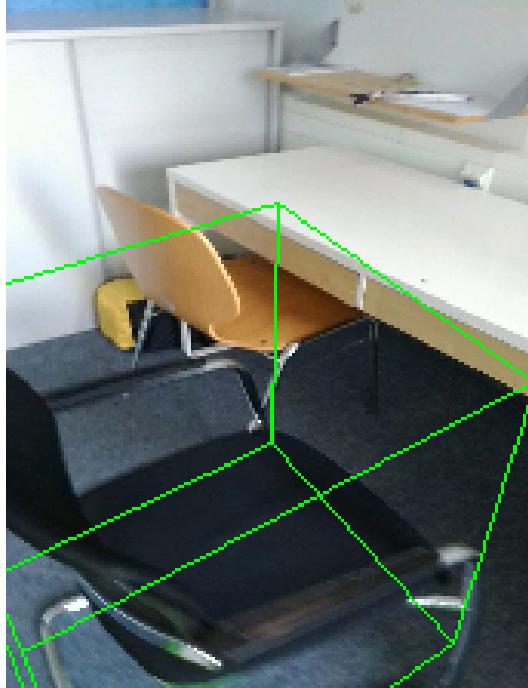


Figure B8: An example of Qwen-generated caption: “A black plastic chair with a cushioned seat and backrest. The frame is metallic, featuring curved legs and armrests. Designed for ergonomic seating in office or classroom settings. Positioned near a desk with papers and books, suggesting a workspace environment.”

Analyze the object in the green bounding box across multiple viewpoints. Generate a caption with:

- Category**:
 - Use specific name if confident (e.g., "mug")
 - Use "generic-type object" for uncertain cases (e.g., "container-type object")
 - Flag low-confidence predictions with "possibly"
- Attributes**:
 - Color patterns & material properties
 - 3D shape characteristics & structural features
 - Functional affordances
 - Contextual placement & surrounding objects
- Confidence Signals**:
 - "The tapered rim suggests..."
 - "While resembling a vase, the presence of..."
 - "Inconclusive evidence for..."

Output template:
 "A [material] [confidence][category] with [color] and [shape]. [Structure/texture details]. [Function inference]. [Contextual placement]."

Examples:

- High Confidence**: "A glossy ceramic mug with deep blue coloring and rounded shape. Has a comfortable handle and flat base. Made for holding hot drinks. Sitting beside a coffee maker and jar of beans on a kitchen counter."
- Moderate Confidence**: "A possibly glass vase-type object with translucent amber coloring. Fluted body shape and water droplets on surface. Likely floral display container. Found on windowsill with plants and pruning shears nearby."
- Low Confidence**: "A metallic tool-type object, matte silver with angular grooves. Ambiguous function between wrench or specialized clamp. Seen in workshop environment near assembly parts."

Figure B9: Prompts for Qwen generating object captions.

Table B3: Results are presented in $\text{Acc}@0.5\text{IoU}$ on Anywhere3D-Bench. *object bbox* in the table denotes the ground-truth object locations and sizes for simplicity. *Chat-Scene evaluation is only conducted on ScanNet. **Human performance is evaluated on a subset of 200 expressions obtained through stratified random sampling across four levels.

	Open Source	Area Level	Space Level	Object Level	Part Level	Overall
LLMs: <i>object bbox, captions</i>						
GPT-4.1	✗	51.85 ± 1.50	10.10 ± 0.19	45.81 ± 0.30	11.52 ± 1.65	26.26 ± 0.16
o4-mini	✗	53.70 ± 2.62	11.33 ± 0.38	46.60 ± 0.22	11.53 ± 0.18	27.18 ± 0.25
Qwen3-32B	✓	30.51 ± 1.62	7.28 ± 0.29	38.40 ± 0.42	7.08 ± 0.15	20.20 ± 0.22
Qwen2.5-72B	✓	25.22 ± 1.22	3.66 ± 0.19	31.90 ± 0.85	2.42 ± 0.84	15.26 ± 0.51
Qwen2.5-VL-72B	✓	25.14 ± 1.12	2.94 ± 0.06	28.09 ± 1.48	2.33 ± 0.73	13.56 ± 0.76
DeepSeek-R1-671B	✓	45.50 ± 1.40	8.94 ± 0.27	45.98 ± 0.24	9.58 ± 0.26	25.09 ± 0.22
MLLMs: <i>object bbox, captions, BEV, video frames</i>						
GPT-4.1	✗	54.50 ± 0.74	12.10 ± 0.06	51.36 ± 0.89	15.02 ± 0.73	29.81 ± 0.30
o4-mini	✗	54.50 ± 1.50	14.50 ± 0.13	53.78 ± 1.34	17.62 ± 0.37	32.04 ± 0.35
LLaVA-OneVision-7B	✓	4.76	1.18	7.02	0.52	3.46
Qwen2.5-VL-72B	✓	24.52 ± 1.10	5.23 ± 0.29	38.89 ± 0.36	4.75 ± 0.30	18.74 ± 0.22
GPT4Scene	✓	4.23	4.08	24.21	3.89	11.36
3D visual grounding models: <i>point clouds, video frames</i>						
PQ3D	✓	11.82 ± 1.33	4.23 ± 0.14	23.52 ± 0.43	2.76 ± 0.54	11.55 ± 0.04
3D-VisTA	✓	12.35 ± 0.31	7.16 ± 0.36	23.86 ± 0.48	2.85 ± 0.90	11.55 ± 0.15
Chat-Scene*	✓	27.24 ± 0.62	3.06 ± 0.33	30.12 ± 0.48	3.74 ± 0.00	17.28 ± 0.22
Human**	–	100.00	82.00	98.00	97.00	91.00

Table B4: Results are presented in $\text{Acc}@0.75\text{IoU}$ on Anywhere3D-Bench. *object bbox* in the table denotes the ground-truth object locations and sizes for simplicity. *Chat-Scene evaluation is only conducted on ScanNet. **Human performance is evaluated on a subset of 200 expressions obtained through stratified random sampling across four levels.

	Open Source	Area Level	Space Level	Object Level	Part Level	Overall
LLMs: <i>object bbox, captions</i>						
GPT-4.1	✗	26.98 ± 0.74	4.08 ± 0.13	40.98 ± 0.29	5.70 ± 0.37	19.34 ± 0.27
o4-mini	✗	30.69 ± 0.00	4.35 ± 0.13	42.19 ± 0.52	6.22 ± 0.37	20.23 ± 0.18
Qwen3-32B	✓	11.99 ± 1.10	2.60 ± 0.34	34.98 ± 0.26	3.25 ± 0.36	15.11 ± 0.16
Qwen2.5-72B	✓	5.11 ± 1.86	1.00 ± 0.24	28.76 ± 1.13	1.64 ± 0.15	11.45 ± 0.57
Qwen2.5-VL-72B	✓	6.08 ± 0.37	0.96 ± 0.06	25.47 ± 1.48	1.55 ± 0.00	10.30 ± 0.59
DeepSeek-R1-671B	✓	23.99 ± 1.53	3.81 ± 0.32	41.40 ± 0.21	5.09 ± 0.15	19.07 ± 0.14
MLLMs: <i>object bbox, captions, BEV, video frames</i>						
GPT-4.1	✗	27.51 ± 4.50	4.80 ± 0.26	45.91 ± 0.30	7.38 ± 0.55	21.72 ± 0.46
o4-mini	✗	32.54 ± 0.37	5.53 ± 0.38	48.42 ± 1.04	8.81 ± 0.00	23.48 ± 0.16
LLaVA-OneVision-7B	✓	0	0.27	5.56	0	2.13
Qwen2.5-VL-72B	✓	3.88 ± 1.10	2.06 ± 0.14	34.63 ± 0.24	2.76 ± 0.15	14.10 ± 0.12
GPT4Scene	✓	2.12	0.18	18.34	0	6.88
3D visual grounding models: <i>point clouds, video frames</i>						
PQ3D	✓	4.23 ± 1.06	0.45 ± 0.09	20.20 ± 0.54	0.00 ± 0.00	7.81 ± 0.15
3D-VisTA	✓	3.35 ± 0.31	0.33 ± 0.05	21.35 ± 0.40	0.00 ± 0.00	8.11 ± 0.11
Chat-Scene*	✓	12.19 ± 0.62	0.43 ± 0.00	26.54 ± 0.33	0.00 ± 0.00	13.23 ± 0.12
Human**	–	100.00	48.00	97.00	83.00	74.00

These results underscore the importance of reasoning capabilities in effectively addressing our benchmark.

Table B5: Evaluation between thinking and non-thinking models on the *Anywhere3D-Bench*. Specifically, we compare Qwen3-32B in its thinking and non-thinking modes, as well as DeepSeek-R1 v.s. DeepSeek-V3. Results are reported in terms of $\text{Acc}@0.25\text{IoU}$, $\text{Acc}@0.5\text{IoU}$, and $\text{Acc}@0.75\text{IoU}$.

	Open Source	Area Level	Space Level	Object Level	Part Level	Overall
Acc@0.25IoU						
Qwen3-32B(non-thinking)	✓	54.67 ± 1.33	9.34 ± 0.48	31.97 ± 0.73	14.08 ± 0.54	21.49 ± 0.15
Qwen3-32B(thinking)	✓	59.79 ± 3.70	12.15 ± 0.39	40.18 ± 0.48	19.17 ± 1.44	26.76 ± 0.44
DeepSeek-V3-671B	✓	61.38 ± 1.91	9.58 ± 1.03	41.06 ± 0.81	18.48 ± 1.88	26.01 ± 0.72
DeepSeek-R1-671B	✓	71.96 ± 1.40	13.93 ± 0.82	47.76 ± 0.12	24.79 ± 1.05	31.95 ± 0.53
Acc@0.5IoU						
Qwen3-32B(non-thinking)	✓	20.46 ± 1.10	5.44 ± 0.16	30.40 ± 1.00	4.32 ± 1.30	15.40 ± 0.25
Qwen3-32B(thinking)	✓	30.51 ± 1.62	7.28 ± 0.29	38.40 ± 0.42	7.08 ± 0.15	20.20 ± 0.22
DeepSeek-V3-671B	✓	26.63 ± 0.80	6.05 ± 0.69	39.52 ± 0.74	6.13 ± 0.84	19.67 ± 0.50
DeepSeek-R1-671B	✓	45.50 ± 1.40	8.94 ± 0.27	45.98 ± 0.24	9.58 ± 0.26	25.09 ± 0.22
Acc@0.75IoU						
Qwen3-32B(non-thinking)	✓	5.82 ± 0.92	1.87 ± 0.14	27.46 ± 0.86	1.90 ± 1.05	11.44 ± 0.17
Qwen3-32B(thinking)	✓	11.99 ± 1.10	2.60 ± 0.34	34.98 ± 0.26	3.25 ± 0.36	15.11 ± 0.16
DeepSeek-V3-671B	✓	8.82 ± 1.10	2.17 ± 0.47	35.50 ± 1.04	2.50 ± 0.60	14.78 ± 0.46
DeepSeek-R1-671B	✓	23.99 ± 1.53	3.81 ± 0.32	41.40 ± 0.21	5.09 ± 0.15	19.07 ± 0.14

B.6 Detailed Analysis on Area Level

At the area level, we further categorize referring expressions into two types. The first type is *Objects Combination*, where most of the relevant objects are explicitly mentioned in the expression. For example, “Identify the conference area with the long rectangular wooden table surrounded by chairs, used for meetings and discussions.” This expression explicitly refers to the area formed by the table and surrounding chairs. The second type is *Commonsense Reasoning*, where models are required to apply commonsense knowledge to infer implicitly indicated objects before identifying the corresponding area. For instance, “Choose the conference area suitable for holding face-to-face meetings.” the expression does not directly mention the objects, and the model must first deduce the components that constitute such a conference area.

Table B6: Analysis on area level

Model	LLM setting			VLM setting		
	Qwen2.5-72B	Qwen3-32B	DeepSeek-R1-671B	GPT-4.1	o4-mini	Qwen2.5-VL-72B
Object Combination	66.15	64.62	84.62	95.38	<u>87.69</u>	64.62
Commonsense Reasoning	58.06	53.23	66.94	76.61	<u>72.58</u>	53.22

Table B6 demonstrates the performance of six top models on two types of expressions at area level. All models exhibit weaker performance on expressions that necessitate commonsense reasoning for the initial identification of the target objects, illustrating their limitations in applying commonsense knowledge within 3D scenes.

B.7 Evaluation Cost

The inference cost varies significantly across models, with DeepSeek-R1-671B costing approximately \$40, GPT-4.1 \$53, o4-mini \$120, and Qwen3-32B around \$9 per full evaluation on *Anywhere3D-Bench*.

C How Can We Improve MLLMs’ Ability on Multi-level Visual Grounding?

C.1 Error Analysis of Bounding Box Predictions

For the incorrect bounding boxes predicted by GPT-4.1, we first aim to analyze whether the error primarily arises from inaccuracies in the size or the position of the bounding boxes, with particular

focus on the two challenging visual grounding levels, i.e., space level and part level. We set both the predicted and ground-truth bounding box positions to the origin (0, 0, 0) and compute $\text{Acc}@0.25\text{IoU}$. This allows us to assess how many predictions fail primarily due to incorrect size estimation, as illustrated in Table C1

Table C1: Error analysis of GPT-4.1’s bounding box predictions. We report $\text{Acc}@0.25\text{IoU}$ under two settings: (1) full IoU considering both location and size (“location + size”), the same setting reported in our main paper, and (2) IoU computed by aligning both predicted and ground-truth boxes at (0, 0, 0) to evaluate only size accuracy (“size”).

Model	area	space	object	part	overall
GPT-4.1(location + size)	81.48 ± 2.25	18.95 ± 0.64	53.88 ± 1.04	29.02 ± 0.73	37.58 ± 0.37
GPT-4.1(size)	94.18 ± 0.75	88.85 ± 0.38	78.36 ± 0.81	64.51 ± 0.37	81.86 ± 0.46

The evaluation results reveal that GPT-4.1 achieves relatively high accuracy in predicting bounding box sizes—88.85% at the space level and 64.51% at the part level. The substantial increase in accuracy—from 18.95% to 88.85% at the space level, and from 29.02% to 64.5% at the part level—demonstrates that the majority of GPT-4.1’s failures at these two levels can be attributed to inaccurate localization rather than size estimation.

Furthermore, we evaluate cases in which the predicted bounding boxes completely deviate from the ground truth—i.e., there is no spatial intersection between the two. To quantify whether any overlap exists between the predicted and ground-truth bounding boxes, we compute the metric $\text{Acc}@> 0, \text{IoU}$, as reported in Table C2. Notably, at the space level, approximately 70% of the predictions exhibit no overlap with the ground truth. This finding highlights that even the top-performing model struggles to accurately comprehend and reason about spatial configurations at the space level.

Table C2: GPT-4.1 performance measured by $\text{Acc}@> 0 \text{IoU}$. Under this metric, a prediction is considered correct if there is any non-zero intersection between the predicted bounding box and the ground-truth bounding box.

Model	area	space	object	part	overall
GPT-4.1	90.48 ± 0.75	30.74 ± 0.64	65.00 ± 0.45	58.42 ± 0.55	51.50 ± 0.40

C.2 Object Orientation Generated by Orient-Anything

In this section, we detail the process of generating object orientations using Orient Anything.

For each object in the scene graph, we first leverage meta-information from the video to select video frames capturing it from different viewpoints. Then we feed these frames into Orient Anything, which outputs predicted azimuth angle between the camera pose and the object, along with corresponding confidence scores. Then, for each video frame of the object, we combine the camera extrinsic parameters, the azimuth angle predicted by Orient Anything, and the scene coordinate system to compute the object’s orientation in that frame. The orientation is classified into one of five categories: “positive x”, “positive y”, “negative x”, “negative y”, or “not sure”. The “not sure” label is assigned when (i) the object’s orientation is clearly not aligned with x-axis or y-axis, (ii) the object has no meaningful orientation (e.g., a circular footstool), or (iii) the confidence score predicted by Orient Anything is below 0.9.

We then apply majority voting across all video frames of the object to determine its final orientation, selecting from one of the five predefined categories, i.e. “positive x”, “positive y”, “negative x”, “negative y”, or “not sure”.

As illustrated in Fig. C1, the ground-truth orientation of chair-1 is negative x. We first utilize Orient Anything to achieve its orientation in each frame. Then decide its final orientation through majority voting of these frames.

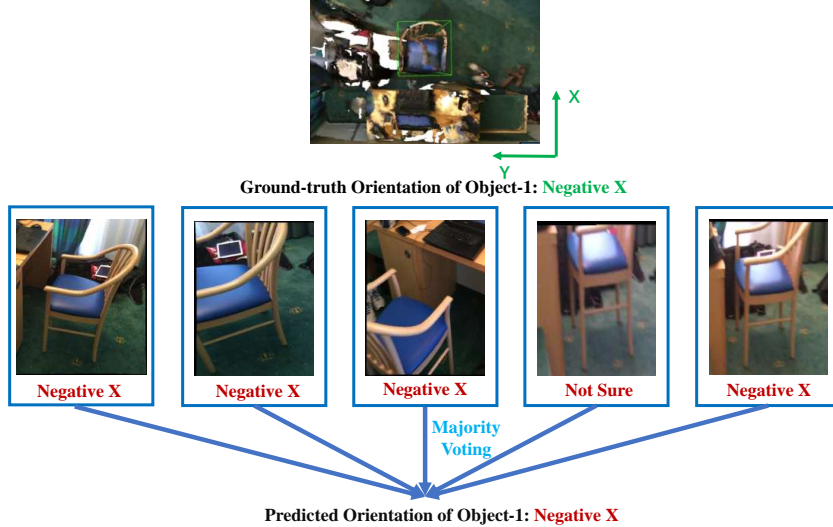


Figure C1: ground-truth orientation of object-1 and the predicted orientation of object-1 by Orient Anything.

C.3 More results on Visual Perception and Relational Reasoning Enhancement

We apply visual perception enhancement (human-selected key frames) and relational reasoning enhancement (BEV images with coordinate axes and object orientations predicted by Orient Anything) **jointly** to evaluate model performance under both enriched input enhancements. In addition, we manually annotate the object orientations in the scenes and use them as alternative inputs to compare model performance against predicted orientations from Orient-Anything, under the same enhancement settings.

Table C3: Effect of the visual perception enhancement and the relational reasoning enhancement, and visual perception and relational reasoning **jointly**. Δ denotes the change in accuracy relative to GPT-4.1. The reported results are based on the human evaluation subset and averaged across three independent trials.

Method	Area	Space	Object	Part	Overall
<i>GPT-4.1</i>	86.67	15.29	54.29	33.33	37.00
Δ (GPT-keyframe)	4.44 ↓	2.75 ↑	2.86 ↓	8.90 ↑	1.00 ↑
Δ (Human-keyframe)	6.66 ↑	7.85 ↑	3.33 ↑	15.57 ↑	7.50 ↑
Δ (BEV-axes)	6.66 ↑	1.96 ↑	2.85 ↑	5.56 ↑	3.00 ↑
Δ (BEV-axes + ori.)	2.22 ↑	5.49 ↑	0.96 ↓	3.34 ↑	4.00 ↑
Δ (Human-keyframe + BEV-axes + ori.)	6.66 ↑	10.59 ↑	1.42 ↑	15.57 ↑	7.83 ↑
Δ (Human-keyframe + BEV-axes + human ori.)	4.44 ↑	9.41 ↑	5.24 ↑	15.57 ↑	8.50 ↑

As shown in Table C3, applying both visual and relational enhancements leads to performance gains across all grounding levels compared to the baseline GPT-4.1. However, when compared to using only the *human-keyframe* visual enhancement, the addition of relational enhancement—even when using manually annotated orientations—does not yield a significant further improvement in performance at space level. Although object orientations and coordinate axes provide GPT-4.1 with richer spatial information, we suspect that the model struggles to correctly interpret and utilize this information. In particular, it appears to have difficulty reasoning about spatial relationships involving transformations between ego-centric views, object orientations, and the global coordinate system.

To further assess the model’s understanding and reasoning of spatial information including object orientation, ego-centric views and global coordinate system, we design an experiment to evaluate GPT-4.1’s ability to interpret object orientations and perform spatial relationship transformations.

Specifically, we prompt the model with a question using the following template Fig. C2, where $axes \in \{+x, -x, +y, -y\}$ and $direction \in \{\text{left}, \text{right}\}$:

Suppose the refrigerator’s orientation is *axes* direction. If you are facing the refrigerator and using a right-handed coordinate system, which direction does your *direction* side point to (+x, -x, +y, or -y)?

Figure C2: Question template to test GPT-4.1 understanding on spatial information including orientation, ego-centric view and spatial relationship transformation.

Table C4: GPT-4.1’s understanding on spatial orientations and spatial relationship transformations.

orientation of the refrigerator	direction	ground-truth answer	GPT-4.1 answer	correct reasoning process?
-x	left	+y	+y	✗
-x	right	-y	-y	✗
+x	left	-y	+y	✗
+x	right	+y	-y	✗
-y	left	-x	-x	✗
-y	right	+x	-x	✗
+y	left	+x	-x	✗
+y	right	-x	+x	✗

The ground-truth answers and those answers provided by GPT-4.1 are presented in Table C4. The results indicate that the model struggles with spatial relationship transformations. Even in cases where the final answer is correct, the underlying reasoning process is often flawed—for instance, the model may arrive at the correct answer by making two offsetting transformation errors. This observation helps explain why GPT-4.1 continues to struggle with relational reasoning at the space level, even when provided with manually annotated object orientations and axes in BEV.

C.4 Detailed Analysis on Qualitative Results

Here, we provide a detailed analysis of the qualitative results. As illustrated in Fig. C3, Fig. C4, Fig. C5, and Fig. C6, ground-truth bounding boxes are shown in green, while GPT-4.1’s predicted bounding boxes are shown in red. In the “Reasoning” section below each example, the incorrect reasoning steps are underlined in red.

In Example (a), GPT-4.1 fails to correctly interpret the spatial relationship: the right side of the piano should correspond to the direction of decreasing x in the coordinate system. Additionally, the model places the small speaker on the floor rather than on top of the piano, which violates commonsense knowledge.

In Example (b), although GPT-4.1 roughly identifies the correct location of the clock, it misunderstands the orientation in which the clock is placed. The term *thickness* should refer to the extent to which the clock protrudes from the wall. A wall-mounted clock should be vertically aligned against the wall, rather than lying flat.

In Example (c), the primary mistake made by GPT-4.1 lies in its misinterpretation of the sofa’s orientation. The orientation of a sofa should correspond to the direction a person would face when standing up from it. Additionally, the model made a minor error in identifying the starting point—it should be the midpoint of the front edge of the sofa, rather than its geometric center.

In Example (d), although GPT-4.1 correctly identifies the cabinet and recognized that the two compartments are distributed on the left and right sides along the y-axis, it still makes an error in spatial reasoning by failing to correctly map the concept of "left" and "right" to the corresponding directions of the coordinate axis.

In Example (e), GPT-4.1 simply treats the bottommost drawer as the cabinet (i.e., object-16). The lack of fine-grained visual details makes it difficult for the model to identify the white drawer located at the bottom of the cabinet.

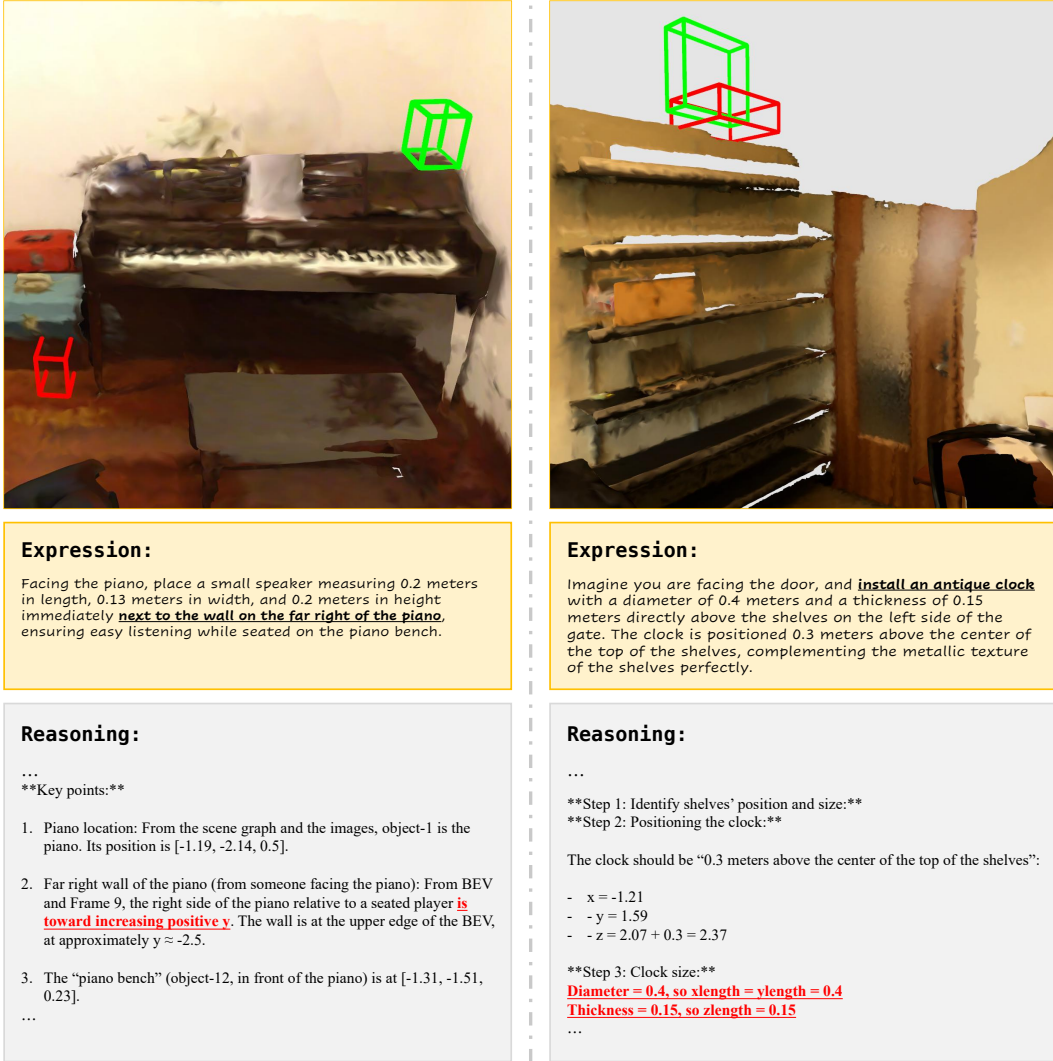


Figure C3: Reasoning process of qualitative examples (a: left) (b: right).

In Example (f), GPT-4.1 makes errors in translating spatial relationships into coordinate-based representations and also fails to identify an object that is placed on the floor.

In Example(g), GPT-4.1 correctly identifies the two white chairs and its mathematical calculations are precise. However, the method it uses to compute the distance between the two objects in space is inappropriate. Rather than using the distance between their center points, the calculation should follow commonsense reasoning—in this context, it should be the shortest distance between the two objects on the XY plane.,

In Example (h), GPT-4.1 correctly identifies sofa-1, coffee table-2, and sofa-4 along with their respective positions. However, a typical arrangement for 2–3 friends to sit, drink tea, and chat would usually involve being seated on the same sofa, since the distance between sofa-1 and sofa-4 exceeds 3.5 meters.

D Limitations and Future Directions

In this section, we outline the limitations of our current work and propose directions for future research.

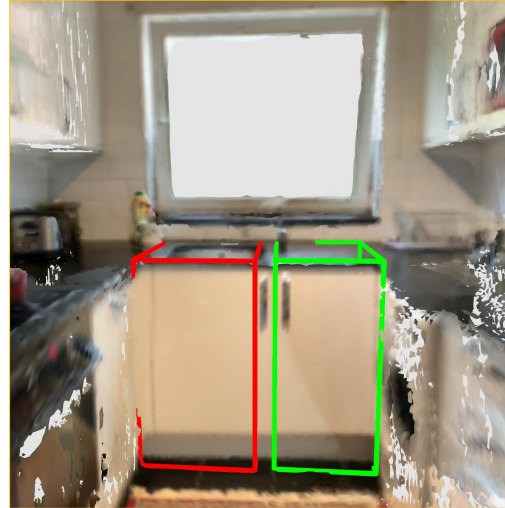


Expression:

Standing up from the middle of the sofa closer to the door, walk 1.5 meters **forward** and then **turn right**. Walk another 1 meter forward and stop. Place a trash bin with 0.3 meters in both width and length and 0.45 meters in height centered at the current position.

Reasoning:

...
 ### 1. Identify the starting point:
 the middle of the sofa closer to the door
 - The BEV shows the door is at the bottom-right, into the corridor/foyer (where object-10 is close by).
 - The sofa closer to this door is **object-1**, based on both position and BEV layout.
 ### 2. Find the center coordinate and orientation:
 - **Object-1 center:** (-0.11, 0.12, 0.64), size: [1.08, 1.63, 0.78]
 - The **middle** of the sofa is its center: (-0.11, 0.12, 0.64)
 #### Orientation: What does "forward" mean?
 - "Walk forward" implies moving toward the front of the sofa if you are "standing up from it," most logically in the direction you'd be facing as you stand from sitting towards the room (**towards positive y**).
 ...



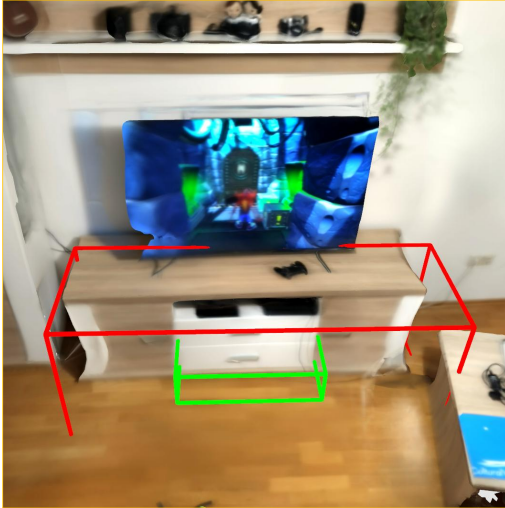
Expression:

Select the compartment of the cabinet below the window, where **the door opens to the right**.

Reasoning:

...
 1. **Identifying the Cabinet Below the Window:**
 - From the scene graph, object-8 is described as: "A white cabinet with a rectangular... Features two doors with vertical handles. Likely used for storage in the kitchen. Positioned below a countertop, adjacent to a sink and near other kitchen appliances." matching object-8.
 2. **Identifying the Correct Compartment (Right Door):**
 - Object-8, from both the BEV and 2D images, consists of two compartments (left and right doors). The rightmost compartment is the one whose door opens to the right.
 - Since object-8 has the position [2.0, 0.15, 0.58] and size [0.62, 0.98, 0.89], and has two doors, each door is roughly half the cabinet's y-size.
 3. **Predicting the 3D Bounding Box for the Right Compartment:**
 - Center of the whole cabinet (object-8): [2.0, 0.15, 0.58].
 - Cabinet total y-length: 0.98 m. Each compartment y-length: $0.98 / 2 = 0.49$ m.
 - **The right door is positioned at the higher y-value** (since in front view, right side = higher y, matching with other object placements in the BEV image).
 ...

Figure C4: Reasoning process of qualitative examples (c: left) (d: right).



Expression:

Pull the white drawer at **the bottommost level** directly below the TV outward by 0.25 meters.

Reasoning:

- ...
1. The TV is object-15, positioned at [0.12, -1.44, 2.66] with size [1.17, 0.19, 0.79].
 2. Directly below the TV, the most likely candidate for a bottommost white drawer is object-16
 3. The TV stand/cabinet, seen in the 2D images (frames 4 and 6), confirms the structure has drawers. **The bottommost drawer is the one closest to the floor, matching object-16.**
 4. The referring expression says to pull the drawer outward by 0.25 meters. Outward here means in the +y direction (since drawers pull towards the viewer, who would be facing the TV from the main open part of the room/audience in the BEV).
- ...



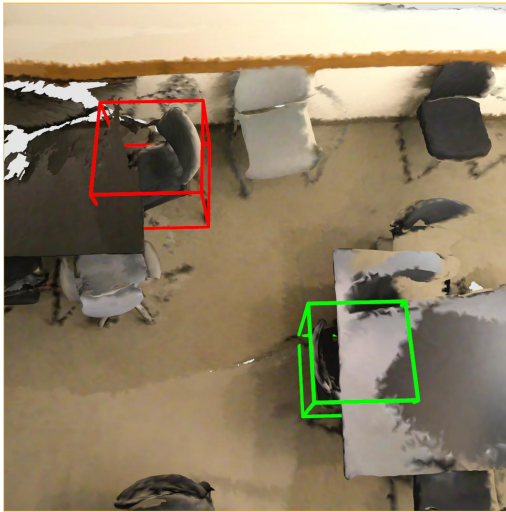
Expression:

Standing up from the armchair and walking 1 meter forward, which object on the floor **directly to my right** is against the wall?

Reasoning:

- ...
1. ****Locate the armchair**:**
 - From the BEV and scene graph, 'object-10' ("A woven wicker chair...") is the likely armchair. Its position is [-0.97, 1.85, 0.7].
 2. ****User walks 1 meter forward**:**
 - Forward from the armchair (based on typical room orientation and BEV layout) would likely be decreasing y (since the opening toward the rest of the room is in that direction).
 - So, new approximate position: [-0.97, 0.85, 0.7]
 3. ****Object to the right, on the floor, and against the wall from this new position**:**
 - "To the right" relative to the forward direction is toward increasing x.
 - Let's look at candidate objects near [-0.97, 0.85, 0.7] with greater x and next to the wall.
 - Reviewing the scene graph, these are the possible candidates:
 - object-5: position [-1.8, 0.96, 1.05]
 - object-6: position [-1.81, 0.96, 1.84]
 - Now, with BEV confirmation:
 - The wall on the right after walking forward from the armchair (by 'object-10') would be the right-hand wall, where 'object-5' is closely positioned along the wall and **is on the floor (bookshelf base).**
- ...

Figure C5: Reasoning process of qualitative examples (e: left) (f: right).



Expression:

Locate the black chair that is 1 meter away from both white chairs.

Reasoning:

...
 1. Identify the white chairs in the scene
 Based on the scene graph, only two objects plausibly correspond to white chairs:
 - **object-9**: ...
 - **object-39**: ...

Positions:
 - object-9: [-1.87, -0.45, 0.4]
 - object-39: [-0.87, -1.48, 0.37]

2. Find the black chair that is 1 meter from both object-9 and object-39
 Let's compute Euclidean distances (planar, ignoring z for simplicity, as z is the vertical):

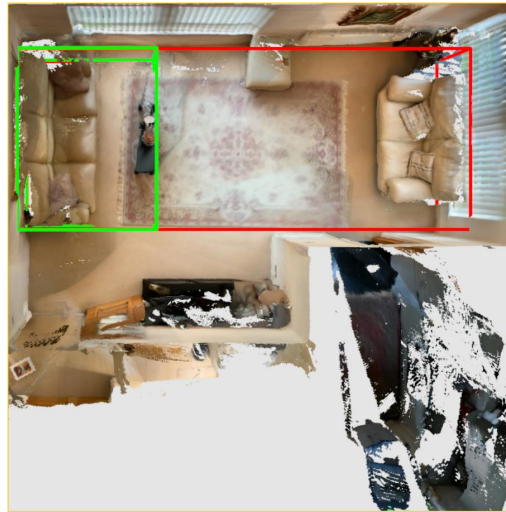
For each black chair:
Candidate 1: object-40 ([caption: dark gray upholstery])
 - Position: [-1.53, -1.24]
Distance to object-9:
 - $\sqrt{(-1.53 - -1.87)^2 + (-1.24 - -0.45)^2} = \sqrt{(0.34)^2 + (-0.79)^2} \approx \sqrt{0.12 + 0.624} \approx \sqrt{0.744} \approx 0.86$ m
Distance to object-39:
 - $\sqrt{(-1.53 - -0.87)^2 + (-1.24 - -1.48)^2} = \sqrt{(-0.66)^2 + (0.24)^2} = \sqrt{0.4356 + 0.0576} \approx \sqrt{0.493} \approx 0.70$ m

So, object-40 is close to both, but not exactly 1 m.

...
Candidate 10: object-24 ([caption: black coloring])
 - Position: [-0.32, -0.08]
Distance to 9: [-0.32 + 1.87 = 1.55], [-0.08 + 0.45 = 0.37]
 - $\sqrt{2.4025 + 0.1369} \approx \sqrt{2.539} \approx 1.59$ m
Distance to 39: [-0.32 + 0.87 = 0.55], [-0.08 + 1.48 = 1.4]
 - $\sqrt{0.3025 + 1.96} \approx \sqrt{2.2625} \approx 1.50$ m
 Still too far.

Given the ambiguity of scene size and natural tolerance, object-40 is best matching.

...



Expression:

Select an area suitable for brewing tea, drinking tea, and chatting with two or three friends.

Reasoning:

...
****Requirements Breakdown:****

Space for making and drinking tea, and sitting comfortably together.
 - Needs seating for 2 or 3 people, a coffee table for serving tea, and a relaxed social setting.

****Analysis:****
 - The living room space in the BEV shows two sofas (object-1 and object-4), a coffee table (object-2), and a rug creating a gathering area.
 - Object-2 (coffee table) in the scene graph is described as having a mug, a bowl of fruit, and a plate which fits the brewing and drinking teapurpose.
 - **Object-1 and object-4 are beige sofas placed across and adjacent to the coffee table**, offering social seating.
 - The surrounding area (including the rug) forms the ideal interaction space for relaxing and chatting, rather than the kitchen area at the top left with the fridge and appliances.

...

Figure C6: Reasoning process of qualitative examples (g: left) (h: right).

First, we plan to develop a training set for *Anywhere3D-Bench*. This would enable the supervised fine-tuning or reinforcement learning-based fine-tuning strategies to enhance the multi-level visual grounding capabilities of both 3D visual grounding models and lightweight VLMs.

Second, we aim to perform a deeper analysis of the reasoning processes produced by models and design corresponding evaluation metrics to assess the correctness of intermediate reasoning steps. In some cases, even if the final bounding box prediction is correct, the intermediate reasoning may involve compensatory errors—e.g., two incorrect steps canceling each other out. To address this, we are hoping to construct dual-form expressions, such as converting “Facing the sofa, place a table on the right side of the sofa” into “Imagine sitting on the sofa, place a table on the left side.” A model’s prediction should only be considered correct if it answers both dual expressions consistently.

Third, while current model outputs are represented as the center coordinates and size of a 3D bounding box, we are interested in exploring a multiple-choice formulation. In this setting, the model would select the correct bounding box from a set of candidates, including the ground-truth and several distractors sampled from the scene.

Fourth, we hope to move beyond visual grounding alone and explore object generation at the grounded location, such as generating corresponding 2D images of objects placed in the predicted 3D position.

Fifth, many expressions in *Anywhere3D-Bench* can naturally serve as instructions. In future work, we plan to extend the benchmark toward embodied tasks, enabling agents (e.g., robots or simulated avatars) to execute the instructions in interactive 3D environments.